

1 A ROS-Ca<sup>2+</sup> signalling pathway identified from a chemical screen for modifiers of sugar-  
2 activated circadian gene expression.

3 Xiang Li<sup>1</sup>, Dongjing Deng<sup>1</sup>, Gizem Cataltepe<sup>1,2</sup>, Ángela Román<sup>1</sup>, Carolina Cassano Monte-  
4 Bello<sup>2</sup>, Aleksandra Skyricz<sup>2</sup>, Camila Caldana<sup>2</sup>, Michael J Haydon<sup>1</sup>

5 1 School of BioSciences, University of Melbourne, VIC, 3010, Australia

6 2 Max Planck Institute of Molecular Plant Physiology, Potsdam-Golm, Germany

7 Corresponding author: Michael J. Haydon [m.haydon@unimelb.edu.au](mailto:m.haydon@unimelb.edu.au) +61 3 8344 6232

8

9

10

11

12

13

14

15

16

17

18

19

20

21

22 **Abstract**

23 Sugars are essential metabolites for energy and anabolism that can also act as signals to  
24 regulate plant physiology and development. Experimental tools to disrupt major sugar  
25 signalling pathways are limited. We have performed a chemical screen for modifiers of  
26 activation of circadian gene expression by sugars to discover pharmacological tools to  
27 investigate and manipulate plant sugar signalling. Using a library of commercially available  
28 bioactive compounds, we identified 75 confident hits that modified the response of a  
29 circadian luciferase reporter to sucrose in dark-adapted seedlings. We validated the  
30 transcriptional effect on a subset of the hits and measured their effects on a range of sugar-  
31 dependent phenotypes for 13 of these chemicals. Chemicals were identified that appear to  
32 influence known and unknown sugar signalling pathways. Pentamidine isethionate (PI) was  
33 identified as a modifier of a sugar-activated  $\text{Ca}^{2+}$  signal that acts downstream of superoxide in  
34 a metabolic signalling pathway affecting circadian rhythms, primary metabolism and plant  
35 growth. Our data provide a resource of new experimental tools to manipulate plant sugar  
36 signalling and identify novel components of these pathways.

37

38 Keywords: circadian clock, sugar signalling, calcium, reactive oxygen species, superoxide,  
39 chemical screen, *Arabidopsis thaliana*, LOPAC

40

41

## 42 Introduction

43 Cells depend on sugars to generate energy and to build the molecules required for cellular  
44 form and function. Sugars can also act as signalling molecules with various roles in  
45 regulating growth and development, physiological processes, metabolic feedback and  
46 modulating abiotic or biotic stress responses (Rolland *et al.*, 2006). Plants generate their own  
47 sugars from photosynthesis. This dependence on light for energy supply creates specific  
48 challenges for plant cells, which must maintain these processes under both predictable and  
49 unpredictable fluctuations in the growth environment. This requires multiple sugar signalling  
50 pathways to coordinate dynamic supply and demand throughout the plant.

51 There are four well-recognised sugar signalling pathways in plants. HEXOKINASE 1  
52 (HXK1) is responsible for the first enzymatic step in glycolysis but has glucose signalling  
53 functions independent of its enzymatic activity (Moore *et al.*, 2003). G-protein signalling  
54 plays a role in extracellular glucose sensing and cell proliferation (Chen *et al.*, 2003; Urano *et*  
55 *al.*, 2012). TARGET OF RAPAMYCIN (TOR) kinase functions in numerous signalling  
56 pathways and is activated under C-replete conditions (Xiong *et al.*, 2013). By contrast, Snf1  
57 RELATED KINASE 1 (SnRK1) is active under C starvation (Baena-González *et al.*, 2007).  
58 SnRK1 activity is inhibited by the signalling sugar trehalose-6-phosphate (T6P) (Zhang *et al.*,  
59 2009), which is very tightly connected to sucrose levels (Figueroa & Lunn, 2016). SnRK1,  
60 and perhaps also TOR, can directly affect activity of transcription factors (Xiong *et al.*, 2013;  
61 Mair *et al.*, 2015). HXK1 can localise to the nucleus and associate with DNA-binding  
62 complexes (Cho *et al.*, 2006).

63 The critical importance of sugar signalling in plant cells makes genetic analysis of these  
64 pathways challenging. Loss-of-function mutants in *TOR* or *T6P SYNTHASE 1 (TPS1)* are  
65 embryo lethal (Eastmond *et al.*, 2002; Menand *et al.*, 2002) and a double mutant in both  
66 catalytic subunits of SnRK1 is not viable (Ramon *et al.*, 2019). Therefore, most studies on  
67 these pathways have used hypomorphic mutants or inducible transgenic lines (Baena-  
68 González *et al.*, 2007; Gómez *et al.*, 2010; Xiong *et al.*, 2013; Belda-Palazón *et al.*, 2020). By  
69 contrast, growth effects in mutants in *HXK1* or *REGULATOR OF G-PROTEIN SIGNALLING*  
70 *1 (RGS1)* are relatively minor, but both mutants are hyposensitive to growth inhibition by  
71 high exogenous sugar (Moore *et al.*, 2003; Chen *et al.*, 2006).

72 Although there is significant overlap between the cellular processes controlled by these sugar  
73 signalling pathways, particularly growth and energy metabolism, there are distinct features of  
74 their signalling outputs. For example, genetic experiments indicate additive effects of *hxk1-3*  
75 and *rgs1-2* mutants (Huang *et al.*, 2015), suggesting functionally distinct pathways. TOR  
76 regulates proteostasis, autophagy and cell cycle control by sugars (Burkart & Brandizzi,  
77 2021), whereas SnRK1 controls responses to energy deprivation and regulation of iron  
78 homeostasis (Peixoto *et al.*, 2021).

79 The circadian clock is a gene regulatory network that integrates external and intrinsic signals  
80 to coordinate biological rhythms according to daily and seasonal changes in the environment.  
81 Photoautotrophic metabolism requires feedback between C availability and the circadian  
82 oscillator to optimise plant growth and fitness. Sugars affect circadian rhythms in  
83 Arabidopsis in several ways. C status contributes to entrainment, the process of setting the  
84 circadian clock (Haydon *et al.*, 2013), and measurement of photoperiod (Liu *et al.*, 2021).  
85 Reduced photosynthesis lengthens circadian period, which can be suppressed by supplying  
86 sugar (Haydon *et al.*, 2013). Period adjustment by sugars requires T6P-SnRK1 signalling  
87 affecting transcription of *PSEUDO RESPONSE REGULATOR 7 (PRR7)* (Frank *et al.*, 2018).  
88 Sugars can also affect amplitude of specific oscillator components. One mechanism occurs by  
89 post-transcriptional control of GIGANTEA (GI) and requires F-box protein ZEITLUPE  
90 (ZTL) (Haydon *et al.*, 2017).

91 Circadian rhythms rapidly dampen in seedlings released into continuous darkness without  
92 supplied sugar. Application of sucrose to dark-adapted seedlings can re-initiate circadian  
93 rhythms and the phase is set according to the time of sugar application (Dalchau *et al.*, 2011).  
94 This transcriptional response to sugar does not require GI and the signalling processes are not  
95 known. This simple assay provides a sensitive technique to define sugar responses in the  
96 absence of light signals. Transcriptome analysis of this response revealed a role for  
97 superoxide, a reactive oxygen species (ROS), in promoting circadian gene expression and  
98 growth by sugar (Román *et al.*, 2021). To further understand this transcriptional response to  
99 sugar, we screened the Library of Pharmacologically Active Compounds (LOPAC; Sigma)  
100 for chemicals that modify the response of a circadian reporter to sucrose in dark-adapted  
101 seedlings. From a list of 75 confident hit compounds, we selected 15 compounds to further  
102 characterise their effects on sugar-dependent processes. We identified two compounds that  
103 contribute to a sugar-activated ROS-Ca<sup>2+</sup> signalling pathway that affects circadian rhythms,

104 primary metabolism and plant growth. Our data provide a resource of pharmacological tools  
105 to manipulate sugar signalling in plants and has revealed opportunities to define new  
106 components of metabolic signalling.

107 **Materials and Methods**

108 *Plant materials and growth conditions*

109 Transgenic reporter lines in *Arabidopsis thaliana* for *COLD*, *CIRCADIAN RHYTHM AND*  
110 *RNA BINDING 2 (CCR2)* promoter:*LUCIFERASE (LUC)* (Doyle *et al.*, 2002), *DARK*  
111 *INDUCIBLE 6 (DIN6)p:LUC* (Frank *et al.*, 2018), *CaMV 35Sp:AEQUORIN (AEQ)* (Dalchau  
112 *et al.*, 2010)*CIRCADIAN CLOCK ASSOCIATED 1 (CCA1)p:LUC* (CS9382), *TIMING OF*  
113 *CAB 1 (TOC1)p:LUC* (Nakamichi *et al.*, 2005) are in Col-0. *35Sp:LUC* (CS9966) is in Ws-2.  
114 The *glucose insensitive 2 (gin2-1)* *abscisic acid 2 (aba2-1)*, *constitutive triple response 1*  
115 (*ctr1-12*) with a *CCA1p:LUC* transgene have been described (Haydon *et al.*, 2013).  
116 *CCA1p:LUC* was introduced by crossing into *g protein alpha subunit 1 (gpa1-4)* (Jones *et al.*,  
117 2003), *gtp binding protein 1 (agb1-4)* (Ullah *et al.*, 2003), and *rgs1-2* (Chen *et al.*, 2003). The  
118 *g-protein gamma subunit 1 (agg1-1) agg2-1 agg3-3* triple mutant (Thung *et al.*, 2012) and  
119 *casein kinase a 1 (cka1-1) cka2-1 cka3-1* triple mutant (Wang *et al.*, 2014).

120 For sterile culture, seeds were surface sterilised (30% (v/v) bleach, 0.02% (v/v) Triton X-  
121 100), washed three times in sterile water and sown on modified Hoagland media (HM)  
122 (Haydon *et al.*, 2012) or half-strength Murashige and Skoog media (½ MS) (Sigma),  
123 solidified with 0.8% (w/v) agar Type M (Sigma). Seeds were chilled for 2 d at 4°C and grown  
124 in 12 h light (80-100  $\mu\text{mol m}^{-2} \text{s}^{-1}$ ):12 h dark at constant 20°C (L:D).

125 *Chemical screen*

126 Seven d old *CCR2p:LUC* seedlings grown in L:D on HM were wrapped in aluminium foil at  
127 dusk. Under dim green light, individual 10 d old seedlings were transferred in the afternoon  
128 to 96 well white LUMITRAC plates (Greiner) containing 250  $\mu\text{l}$  HM with 0.1% DMSO or 25  
129  $\mu\text{M}$  LOPAC chemical (Sigma) and dosed with 1 mM D-luciferin, K<sup>+</sup> salt (Cayman). Eighty  
130 LOPAC chemicals were included in each plate, plus positive and negative controls. Each  
131 plate was prepared in triplicate. After 84 h in darkness (subjective dawn), 25  $\mu\text{l}$  of 10% (w/v)  
132 sucrose or mannitol and luciferase was measured at 1 h intervals for 24 h in the dark using  
133 orbital scan mode in a LUMIstar Omega plate reader fitted with a Microplate stacker (BMG

134 Labtech). HiTSeekR (List *et al.*, 2016) was used to identify compounds that significantly  
135 altered peak luminescence at 12 h after sucrose application after removing 47 data series from  
136 the total 4,224 deemed as false negatives. The raw data was  $\log_2$  transformed and normalised  
137 with robust *z*-score method for general signal difference correction and inter-plate  
138 comparison before calculation of strictly standardised mean difference (SSMD) values.

139 *Luciferase assays*

140 For sugar response assays, 7 d old seedlings grown in L:D on  $\frac{1}{2}$  MS were wrapped in  
141 aluminium foil at dusk. After 72 h, seedlings were transferred to  $\frac{1}{2}$  MS containing chemicals  
142 in 96 well LUMITRAC plates under dim green light and sugars were added 12 h later at  
143 subjective dawn. 1 mM D-luciferin was applied at least 12 h before commencing  
144 luminescence measurements using orbital scan mode in a LUMIstar Omega plate reader with  
145 Microplate stacker (BMG Labtech). Circadian rhythms were measured in 10 d old  
146 *CCA1p:LUC* and *TOC1p:LUC* seedlings grown on  $\frac{1}{2}$  MS in L:D and transferred at Zeitgeber  
147 Time 0 (ZT0) to 25-well imaging plates (Ting *et al.*, 2022) containing media with DMSO or  
148 chemical before imaging luminescence with a Photon Counting System (HRPCS5, Photek) in  
149 continuous light ( $40 \mu\text{mol m}^{-2} \text{s}^{-1}$ ) or continuous low light ( $<10 \mu\text{mol m}^{-2} \text{s}^{-1}$ ) provided by red  
150 (640 nm) and blue (470 nm) LED lights.

151 *Quantitative RT-PCR*

152 Total RNA was extracted from  $\sim$ 30 mg snap frozen tissue with ISOLATE II RNA Plant Kit  
153 (Meridian Bioscience). cDNA was prepared from 0.5  $\mu\text{g}$  DNase-treated RNA in 10  $\mu\text{l}$   
154 reactions of Tetro cDNA synthesis kit (Meridian Bioscience) using oligo(d)T primer. 10  $\mu\text{l}$   
155 PCR reactions were performed in technical duplicate with SensiFAST SYBR No-ROX  
156 (Meridian Bioscience) with 4 ng cDNA and 300 nM primers (Table S1) on a CFX96 Real-  
157 time PCR System (BioRad). Mean PCR reaction efficiencies were calculated for each primer  
158 pair with LinRegPCR (Ruijter *et al.*, 2009) and used to calculate gene expression levels  
159 ( $\text{PCR\_efficiency}^{-\text{Ct}}$ ).

160 *Growth assays*

161 Germination was measured in non-chilled, surface sterilised Col-0 seeds sown onto  $\frac{1}{2}$  MS  
162 with DMSO or chemical and mannitol or sucrose at ZT0 and immediately placed in L:D.  
163 Radicle emergence was scored at 2 or 3 timepoints per day for 4 d. For hypocotyl and root

164 length measurements, Col-0 was grown in L:D on ½ MS for 2 d and transferred to media  
165 containing DMSO or chemical with 30 mM mannitol or sucrose at ZT0, wrapped in  
166 aluminium foil and grown on vertical plates for 5 d. Hypocotyl and root lengths were  
167 measured from photographs with ImageJ (NIH).

168 *Pigment quantification*

169 Chlorophyll was extracted from 12 7 d old seedlings in 250 µl methanol and quantified by  
170 absorbance spectrophotometry (Porra, 1989). Anthocyanin was extracted from 5 9 d old  
171 seedlings in 250 µl methanol:1% (v/v) HCl and quantified by absorbance spectrophotometry  
172 (Chen *et al.*, 2019).

173 *ROS measurements*

174 L-012 luminescence and nitroblue tetrazolium (NBT) staining were performed in dark-  
175 adapted seedlings in liquid ½ MS as described (Román *et al.*, 2021).

176 *Aequorin experiments*

177 For chemical response assays, ~10 8 d old *35Sp:AEQ* seedlings grown in L:D on ½ MS were  
178 transferred before dusk to 100 µl 5 µM coelenterazine h (Cayman) in 96 well LUMITRAC  
179 plates (Greiner). Luminescence was measured at 1 s intervals in the dark from subjective  
180 dawn using orbital scan mode in a LUMIstar Omega plate reader (BMG Labtech) and 50 µl  
181 of DMSO or chemicals were applied with an injector at 30 s for final concentration of 10 µM  
182 DPI or 25 µM PI. After 270 s, 150 µl discharge solution (1 M CaCl<sub>2</sub>, 10 % (v/v) ethanol) was  
183 injected and cytosolic Ca<sup>2+</sup> concentration was calculated (Fricker *et al.*, 1999). For sugar  
184 response assays, ~10 7 d old *35Sp:AEQ* seedlings grown in L:D were transferred to 100 µl  
185 liquid ½ MS with 20 µM coelenterazine at dusk in 96 well LUMITRAC plates (Greiner) and  
186 wrapped in aluminium foil. After 84 h (subjective dawn), 50 µl ½ MS containing DMSO or  
187 chemicals were added for a final concentration of 5 µM DPI or 25 µM PI and luminescence  
188 was measured at 2 min intervals by orbital scan mode in a LUMIstar Omega plate reader  
189 (BMG Labtech). After 1 h, 75 µl sucrose or mannitol was added for a final concentration of  
190 30 mM with DMSO, 5 µM DPI or 25 µM PI and luminescence was measured at 2 min  
191 intervals for 6 h.

192

193 *RNA-Seq*

194 Fourteen d old Col-0 seedlings grown on  $\frac{1}{2}$  MS in L:D were transferred to media containing  
195 DMSO, 10  $\mu$ M DPI, 25  $\mu$ M PI, 12.5  $\mu$ M AEG3482 or 2  $\mu$ M Tyrphostin AG879 at ZT24,  
196 before lights on. Untreated control seedlings were collected at time of transfer and treated  
197 seedlings were collected at ZT2 and snap frozen in liquid N. Total RNA was extracted from  
198 biological triplicates with ISOLATE II RNA Plant kit (Meridian Bioscience). and quantified  
199 and qualified by Agilent 2100 Bioanalyzer, NanoDrop (ThermoFisher) and 1% agarose gel. 1  
200  $\mu$ g total RNA with RIN value above 7 was used for library preparation by Genewiz using  
201 NEBNext® UltraTM RNA Library Prep Kit for Illumina® and NEBNext Poly(A) mRNA  
202 Magnetic Isolation Module (NEB). Size selection of Adaptor-ligated DNA was then  
203 performed using AxyPrep Mag PCR Clean-up (Axygen), and fragments of  $\sim$ 360 bp (with the  
204 approximate insert size of 300 bp) were recovered. Each sample was then amplified by PCR  
205 for 11 cycles using P5 and P7 primers. The PCR products were cleaned up using AxyPrep  
206 Mag PCR Clean-up (Axygen), validated using an Agilent 2100 Bioanalyzer, and quantified  
207 by Qubit 2.0 Fluorometer (Invitrogen). Libraries with different indices were multiplexed and  
208 loaded on an Illumina HiSeq instrument and sequenced using a 2x150bp paired-end (PE)  
209 configuration; image analysis and base calling were conducted by the HiSeq Control  
210 Software (HCS) + OLB + GAPipeline-1.6 (Illumina) on the HiSeq instrument. All libraries  
211  $>20$  M raw reads with Q30 and Q20  $>95\%$  and  $>98\%$ , respectively.

212 SOAPnuke v2.1.0 (Chen *et al.*, 2018) was used to remove adapter sequences and low-quality  
213 reads from the sequencing data. To identify all the transcripts, we used HiSAT2 v2.2.1 (Kim  
214 *et al.*, 2015) to align the sequencing reads to the *Arabidopsis thaliana* Col-0 genome  
215 (TAIR10) and RSEM v1.2.22 (Li & Dewey, 2011) to quantify the gene expression level of  
216 each replicate. The differential expression analysis was performed by NOIseq v2.37.0  
217 (Tarazona *et al.*, 2015). DEGs were defined as  $\log_2$  change  $> 0.6$  and DE probability  $> 80\%$ .

218 *Metabolomics*

219 Fourteen d old Col-0 seedlings grown hydroponically were transferred to liquid  $\frac{1}{2}$  MS  
220 containing DMSO, 10  $\mu$ M DPI, 25  $\mu$ M PI, 12.5  $\mu$ M AEG3482 or 2  $\mu$ M Tyrphostin AG879 at  
221 ZT23. Tissue was collected for five biological replicates for untreated seedlings at ZT23 and  
222 treated seedlings at ZT24 (lights off), ZT1.5, ZT4, ZT8, ZT10.5, ZT12 (lights on), ZT22.5  
223 and ZT24 (lights off) and snap frozen in liquid N. Fifty mg of ground tissue was used for

224 MTBE:methanol:water 3:1:1 (v/v/v) extraction (Giavalisco *et al.*, 2011). The 150  $\mu$ l of the  
225 organic phase was dried and derivatized (Roessner *et al.*, 2001). One  $\mu$ l of the derivatized  
226 samples were analyzed on a Combi-PAL autosampler (Agilent Technologies) coupled to an  
227 Agilent 7890 gas chromatograph coupled to a Leco Pegasus 2 time-of-flight mass  
228 spectrometer (LECO) (Weckwerth *et al.*, 2004). Chromatograms were exported from Leco  
229 ChromaTOF software (version 3.25) to R software. Peak detection, retention time alignment,  
230 and library matching were performed using Target Search R-package (Cuadros-Inostroza *et*  
231 *al.*, 2009).

232 Metabolites were quantified by the peak intensity of a selective mass. Metabolite intensities  
233 were normalized by dividing the fresh-weight, followed by the sum of total ion count as  
234 described previously (Huege *et al.*, 2011; Giavalisco *et al.*, 2011). Principal component  
235 analysis was performed using pcaMethods bioconductor package (Stacklies *et al.*, 2007). The  
236 significances of metabolites were tested by *t*-test.

## 237 **Results**

238 We exploited the re-initiation of circadian gene expression by sugar in dark-adapted seedlings  
239 to evaluate transcriptional sugar responses in *Arabidopsis*. Using a luciferase reporter system,  
240 this provides a sensitive, high-throughput assay to measure plant sugar responses in the  
241 absence of light. Topical application of 30 mM sucrose to dark-adapted seedlings is sufficient  
242 for a robust response of a circadian luciferase reporter *CCR2p:LUC* (Fig. 1a) and generates  
243 similar sugar concentrations to seedlings grown in the light (Fig. 1b). Sucrose is the most  
244 abundant and mobile soluble sugar in plant tissues, although similar reporter activity is also  
245 elicited by glucose, fructose and maltose (Fig. 1c).

246 Numerous sugar-insensitive mutants have been identified in *Arabidopsis* that are resistant to  
247 growth inhibition by high concentrations of sugars in the media. We tested the transcriptional  
248 responses to sucrose in a collection of these mutants using our assay and observed similar  
249 responses to wild-type seedlings (Fig. 1d-f). Notably, these included mutants in *HXK1* and G-  
250 protein signalling, suggesting these sugar signalling pathways are not required for sugars to  
251 reinitiate circadian rhythms in dark-adapted seedlings.

252 To discover new components involved in plant sugar signalling, we performed a high-  
253 throughput screen for chemicals that modify the transcriptional response to sucrose. Dark-  
254 adapted *CCR2p:LUC* transgenic seedlings were treated with sucrose in the presence of 25

255  $\mu$ M of each of 1280 chemicals from LOPAC (Sigma). This collection of commercially  
256 available chemicals have defined targets in mammalian cells, and mostly target signalling  
257 proteins such as receptors, kinases and ion channels. We used HiTSeekR (List *et al.*, 2016)  
258 to calculate strictly standardised mean difference (SSMD) values. A cut-off of  $\pm 1$  identified  
259 146 chemicals that significantly modified the peak reporter activity (Table S2). To generate a  
260 higher confidence list of candidates, we used a stricter SSMD cut-off of  $\pm 1.28$  which  
261 provided a list of 65 inhibitors and 10 enhancers of the reporter response to sucrose (Table 1).

262 Greater than 10% of compounds present in chemical libraries are reported to exhibit  
263 inhibition of luciferase activity (Thorne *et al.*, 2012). We re-screened 104 chemicals from  
264 LOPAC for their effect on luciferase activity at 25  $\mu$ M using *35Sp:LUC* seedlings (Fig. S1).  
265 We identified two compounds that significantly enhanced luciferase luminescence and 11  
266 compounds that significantly inhibited luminescence, indicating these might be false-  
267 positives identified in the primary screen.

268 We selected 15 chemicals (Fig. S2) for further analyses including diphenyleneiodonium  
269 (DPI), which we previously showed inhibits the transcriptional sugar response (Román *et al.*,  
270 2021), 6-methyl-2-(phenylethynyl)pyridine (MPEP), which strongly inhibited *35Sp:LUC*  
271 luciferase (Fig. S1), and AZD8055, a specific inhibitor of TOR (Montané & Menand, 2013),  
272 which is not in LOPAC but has been reported to affect circadian sugar responses in  
273 *Arabidopsis* (Zhang *et al.*, 2019). We generated dose response curves for these 15 chemicals  
274 based on inhibition of *CCR2p:LUC* luminescence in dark-adapted seedlings treated with  
275 sucrose to determine a minimum effective concentration at which >80% inhibition is  
276 achieved (Fig. 2, Fig. S3). Although the primary screen being performed with 25  $\mu$ M,  
277 effective concentrations ranged from 2-50  $\mu$ M for these chemicals. By contrast, the  
278 maximum inhibition of the luciferase reporter achieved for the TOR inhibitor AZD8055 was  
279 only  $\sim 50\%$ .

280 To validate the efficacy of these compounds on the transcriptional response to sugar, we  
281 again measured luciferase luminescence in *35Sp:LUC* seedlings at the minimum effective  
282 concentration determined from the dose curves (Fig. 3a) and measured *CCR2* transcript in  
283 dark-adapted seedlings treated with sucrose using qRT-PCR (Fig. 3b). This confirmed that all  
284 chemicals inhibited the upregulation of *CCR2* transcript by sucrose to some extent, except for  
285 two metabotropic glutamate receptor (mGluR5) inhibitors MPEP and SIB1893, which also  
286 significantly reduced luciferase luminescence in *35Sp:LUC* seedlings. We therefore excluded

287 these two chemicals from further experiments. We also observed that 50  $\mu$ M roscovitine  
288 increased 35Sp:LUC luminescence, despite inhibiting response of *CCR2p:LUC* and *CCR2*  
289 transcript to sucrose.

290 One of the validated chemicals, tetrabromobenzotriazole (TBB), is a mammalian casein  
291 kinase 2 inhibitor. CK2 is a regulator of the circadian clock and another CK2 inhibitor,  
292 dichlorobenzimidazole ribofuranoside (DRB), has been shown to lengthen circadian period in  
293 *Arabidopsis* (Portolés & Más, 2010). We tested whether DRB inhibits the response of  
294 *CCR2p:LUC* to sucrose in dark adapted seedlings and found no effect at the concentrations  
295 tested (Fig. S4a). Similarly, we could not detect a difference in *CCR2* transcript in a *cka1-1*  
296 *cka2-1 cka3-1* mutants compared to wild type using qRT-PCR in the same assay (Fig. S4b).  
297 These data suggest that it is unlikely that TBB inhibits the transcriptional response to sucrose  
298 by targeting CK2 in *Arabidopsis* seedlings.

299 To build a picture of the broader influence of these selected chemicals on sugar-related  
300 processes, we tested their effects on a range of easily measurable phenotypes. Using the pre-  
301 determined minimum effective concentration for each chemical, we tested effects in the  
302 presence or absence of sucrose on germination of dormant seeds (Fig. S5), seedling biomass,  
303 chlorophyll content, hypocotyl length, root growth and anthocyanin content (Fig. S6). We  
304 observed a range of effects of each chemical on these phenotypes but detected similar  
305 patterns for multiple chemicals that might indicate common signalling pathways. To  
306 summarise these patterns, we plotted normalised effects of phenotypes on radar charts and  
307 ranked the chemicals by the sum of effects (Fig. 4a). Based on these radar charts, we noticed  
308 similar phenotypic patterns for DPI and pentamidine isethionate (PI), emodin and SP600125,  
309 and Tyrphostin AG879, DMH4 and ZM39923, which might indicate these chemicals affect  
310 proteins or signalling pathways with closely related functions.

311 We next tested phenotypic interactions between a selected number of chemicals. We  
312 hypothesised that chemicals that affect the same signalling pathway should be non-additive,  
313 whereas chemicals that affect distinct pathway might show a phenotypic interaction in  
314 combination. We germinated seeds on media containing chemicals alone or in combination at  
315 a 50% inhibitory concentration (Fig. 2) and measured biomass of 7 d old seedlings (Fig. 4b).  
316 DPI and PI in combination did not inhibit seedling growth compared to DPI alone, suggesting  
317 they affect the same pathway, consistent with the similar pattern for these chemicals in the

318 radar charts. By contrast, Tyrphostin AG879 significantly suppressed the growth inhibition  
319 by DPI, indicating these chemicals might act on distinct pathways.

320 To measure the broader effects of these four chemicals on gene expression, we treated  
321 seedlings with each chemical at dawn and performed RNA-seq in seedlings after 2 h to  
322 capture short-term transcriptional effects at the beginning of the photoperiod. We identified  
323 1899 differentially expressed genes (DEGs) between ZT0 and ZT2 (DMSO), but we detected  
324 between one and 16 DEGs between DMSO and any chemical (Table S2, Fig. S7a,b). This  
325 might be because the effect of inhibiting sugar signalling at dawn is diminished in the  
326 presence of abrupt light signalling. It's also possible that since superoxide regulated genes are  
327 biased towards dusk (Román *et al.*, 2021), the short-term effect of DPI is minimal around  
328 dawn. Nevertheless, more than two thirds of DEGs in chemical-treated seedlings versus  
329 controls have been previously reported as sugar-regulated genes (Fig. S7b) (Xiong *et al.*,  
330 2013; Ganpudi *et al.*, 2019; Román *et al.*, 2021; Peixoto *et al.*, 2021). *PATHOGEN AND*  
331 *CIRCADIAN CONTROLLED 1 (PCC1)*, which is upregulated after dawn, was identified as a  
332 DEG for DPI, PI and AEG3482, but not Tyrphostin AG879, providing further support that  
333 Tyrphostin AG879 acts on a distinct signalling pathway.

334 Half of the DEGs identified in Tyrphostin AG879-treated seedlings have been reported as  
335 DEGs in a *sesqia2* SnRK1 hypomorphic mutant (Peixoto *et al.*, 2021). We therefore tested  
336 whether Tyrphostin AG879 affects expression of a SnRK1 transcriptional marker, *DARK*  
337 *INDUCIBLE 6 (DIN6)*. Treatment of *DIN6p:LUC* seedlings at dusk with DPI, PI or  
338 AEG3482 either had no effect, or slightly inhibited luciferase luminescence, whereas  
339 Tyrphostin AG879 increased reporter activity (Fig. S7c). This suggests that Tyrphostin  
340 AG879 can activate SnRK1 activity, either directly or indirectly, which is consistent with the  
341 increased expression of SnRK1-regulated markers in Tyrphostin AG879-treated seedlings  
342 (Fig. S7b). An activation of the starvation response triggered by SnRK1 could explain how  
343 Tyrphostin AG879 counteracted the inhibition of seedlings growth by DPI (Fig. 4b).

344 To explore the effect of these four chemicals on primary metabolism, we performed  
345 metabolite profiling over a 24-h time-course following treatment with each chemical (Table  
346 S4). Principal component (PC) analysis of 63 metabolites over eight time-points revealed a  
347 similar trend for all four chemicals in the direction of change compared to DMSO-treated  
348 samples for PC1 and PC2, which together explained between 63-70% of variance (Fig. S8).  
349 The PC plot for Tyrphostin AG879 suggested a more pronounced effect on the primary

350 metabolome around dusk, compared to the other three chemicals, and the effect of DPI  
351 appeared more pronounced than PI and AEG3482.

352 All four chemicals caused a significant increase in the levels of sucrose, fructose and glucose  
353 at more than one time-point. Sucrose was elevated around dawn and glucose and fructose  
354 elevated during the day (Fig 5a). The glycolysis intermediate glucose-6-phosphate was  
355 significantly lower in Tyrphostin AG879-treated seedlings at ZT10 and ZT12 and also  
356 reduced at ZT24 in seedlings treated with DPI and PI (Fig 5b). We observed significant  
357 increases in tricarboxylic acid (TCA) cycle intermediates, particularly citrate and malate,  
358 with the magnitude of the effect increasing with time for all four chemicals (Fig 5c).

359 Branched-chain amino acids valine, leucine and isoleucine have been associated with HXK1  
360 (Ganpudi *et al.*, 2019) and TOR signalling (Cao *et al.*, 2019) but we did not detect notable  
361 changes for any chemical (Fig. 5d). The difference between Tyrphostin AG879 and the other  
362 three chemicals detected around dusk in the PC analysis is likely explained by significantly  
363 reduced levels of amino acids at ZT10.5, particularly methionine, threonine and lysine (Fig.  
364 5e), which are all synthesised from oxaloacetate in the TCA cycle.

365 We have previously shown that DPI inhibits accumulation of superoxide in dark-adapted  
366 seedlings treated with sucrose and affects expression of circadian gene expression (Román *et*  
367 *al* 2021). The similar phenotypic patterns between DPI and PI, suggest they might affect the  
368 same sugar signalling pathway. We measured the effect of DPI and PI on circadian rhythms  
369 using luciferase reporters and observed lengthening of circadian period by both chemicals  
370 (Fig. 6a). This effect is consistent with expectations for inhibition of sugar signalling into the  
371 clock, similar to effects of inhibiting sugar production from photosynthesis (Haydon *et al.*,  
372 2013). However, neither chemical inhibited the shortening of circadian period by sucrose  
373 (Fig. 6b), which operates by a SnRK1-dependent mechanism (Frank *et al.*, 2018).

374 PI is an antagonist of N-methyl-D-aspartate (NMDA) glutamate receptors in mammalian  
375 cells, so we wondered if PI similarly inhibits  $\text{Ca}^{2+}$  signalling in *Arabidopsis*. We measured  
376 the effect of PI on *35Sp:AEQ*, a luminescent reporter for cytosolic  $\text{Ca}^{2+}$  concentration and  
377 observed a rapid shift in internal  $\text{Ca}^{2+}$  in *Arabidopsis* seedlings (Fig. 7a). By contrast, DPI did  
378 not affect *35Sp:AEQ* in these experiments suggesting it does not have an immediate  
379 influence on cytosolic  $\text{Ca}^{2+}$  in these conditions.

380 Since PI strongly affects cytosolic  $\text{Ca}^{2+}$  concentration and inhibits transcriptional response to  
381 sucrose, we tested whether sucrose could induce a change in cytosolic  $\text{Ca}^{2+}$  concentration in  
382 dark-adapted seedlings. Application of sucrose to dark-adapted seedlings elevated 35Sp:AEQ  
383 luminescence compared to mannitol (Fig. 7b). This response was slower than elevation of  
384 superoxide observed in sucrose-treated seedlings (Román *et al.*, 2021). Elevation of cytosolic  
385  $\text{Ca}^{2+}$  concentration by sucrose was attenuated in DPI-treated seedlings. Similarly, although  
386 35Sp:LUC luminescence was higher in PI-treated seedlings, there was no difference between  
387 sucrose and mannitol (Fig. 7b). This is consistent with the targets of these chemicals acting in  
388 the same sugar-activated  $\text{Ca}^{2+}$ -dependent signalling pathway and suggests that the target of  
389 DPI acts upstream of the target of PI.

390 To test whether PI inhibits elevation of superoxide by sucrose, we measured L-012  
391 luminescence and performed nitroblue tetrazolium (NBT) stains in dark-adapted seedlings.  
392 DPI strongly inhibited L-012 luminescence in sucrose-treated seedlings, but PI did not (Fig.  
393 7c). Similarly, NBT stains indicated that, unlike DPI, PI did not prevent sucrose-activated  
394 superoxide accumulation (Fig. 7d). These data indicate that the target of PI acts downstream  
395 of the target of DPI. This supports the results of the 35Sp:AEQ experiments and suggests that  
396 PI inhibits a ROS-activated  $\text{Ca}^{2+}$ -channel acting downstream of NADPH oxidases in sugar  
397 signalling pathway that regulates circadian gene expression.

## 398 **Discussion**

399 We have used a chemical screen for modifiers of an effect of sucrose on the circadian clock  
400 to identify novel experimental tools to manipulate sugar signalling in *Arabidopsis*. From 75  
401 hit molecules, we confirmed the effect of 13 chemicals and completed broad characterisation  
402 of the effects of these chemicals on key sugar-regulated processes including germination,  
403 growth and pigmentation. These experiments captured a broad picture of the patterns of  
404 phenotypic effects of these chemicals to identify potential shared relationships between them.  
405 We selected four chemicals for metabolite and transcriptome profiling, which suggested they  
406 affect at least two distinct pathways. Two compounds, DPI and PI, appear to act on a sucrose-  
407 activated ROS- $\text{Ca}^{2+}$  signalling pathway, which might represent a novel metabolic signalling  
408 pathway in *Arabidopsis* affecting circadian gene expression and growth. Furthermore, this list  
409 of commercially available sugar signalling modifiers provides a resource that could be used  
410 to fill gaps in known and unknown metabolic signalling processes in plants.

411 The effect of Tyrphostin AG879 on the transcriptome suggested that it might be a modifier of  
412 SnRK1 or a SnRK1-related pathway, and we confirmed that this chemical could activate  
413 *DIN6p:LUC*, a reporter of SnRK1 activity. Although the number of DEGs was small in  
414 Tyrphostin AG879-treated seedlings around dawn, this is consistent with the small effect of  
415 *SnRK1 $\alpha$* -overexpression on the transcriptome and the apparently higher activity of SnRK1 at  
416 this time of day (Peixoto *et al.*, 2021). A SnRK1 activator could be expected to inhibit the  
417 transcriptional response of *CCR2p:LUC* to sucrose in C-starved seedlings. Two other  
418 chemicals, DMH4 and ZM39923, had similar patterns of effects to Tyrphostin AG879, so it  
419 is possible that these also influence SnRK1-related signalling. Interestingly, all three  
420 chemicals are tyrosine kinase inhibitors.

421 The TOR kinase inhibitor, AZD8055, is not represented in LOPAC but we included it in our  
422 experiments because it was able to inhibit the transcriptional response to sucrose. Although  
423 the effect on the luciferase reporter was relatively weak, the effect on the transcript was  
424 strong. TOR is activated by sugar availability and influences circadian rhythms in  
425 *Arabidopsis* (Zhang *et al.*, 2019), so it is possible other modifiers of plant TOR signalling  
426 could have been identified in our screen. Based on phenotypic effects, the most similar  
427 chemicals were roscovitine, a cyclin-dependent kinase inhibitor and TBB. Although TBB is a  
428 CK2 inhibitor, it appears this is not the mechanism by which it affects expression of *CCR2* in  
429 our experiments.

430 DPI and PI have very similar effects on the phenotypes we measured and their inhibition of  
431 growth is not additive, suggesting they act on the same pathway. DPI inhibits accumulation  
432 of superoxide in sucrose-treated seedlings, most likely by inhibiting NADPH oxidases at the  
433 plasma membrane (Román *et al.*, 2021). PI is a NMDA receptor antagonist and therefore  
434 might target a  $\text{Ca}^{2+}$  channel in plant cells. Consistent with this, we found that PI induces a  
435 rapid change in cytosolic  $\text{Ca}^{2+}$  concentration. Application of sucrose to dark-adapted  
436 seedlings elevated cytosolic  $\text{Ca}^{2+}$ , with a slightly slower response than the accumulation of  
437 superoxide. Since PI did not inhibit sucrose activated superoxide accumulation, these results  
438 suggest that the  $\text{Ca}^{2+}$  signal acts downstream of the superoxide signal and that PI targets a  
439 ROS-activated  $\text{Ca}^{2+}$  channel. CYCLIC NUCLEOTIDE GATED  $\text{Ca}^{2+}$  CHANNELs (CNGCs)  
440 and ANNEXINs have been proposed to fulfil this role in plants (Demidchik, 2018).  
441 GLUTAMATE LIKE RECEPTORs (GLRs) have been shown to act upstream of NADPH

442 oxidases (Kong *et al.*, 2016). All these channels are members of large protein families, so  
443 genetic verification of any of these as the targets of PI will be challenging.

444 If our results suggest a novel sugar signalling pathway, a critical question is how the sugar is  
445 sensed. Since NADPH oxidases are present on the plasma membrane, this could be an  
446 extracellular sugar sensing mechanism. A role for RGS1 seems unlikely, since G-protein  
447 mutants are not affected in the sucrose response assay. Receptor-like kinases have been  
448 implicated in numerous extracellular signalling pathways, upstream of NADPH oxidases.  
449 This is a very large protein family, but many of these contain sugar-binding lectin domains  
450 (Sun *et al.*, 2020). However, NADPH oxidases can be triggered by intracellular domains, so  
451 it's also possible that sugars are sensed within cells. Alternatively, DPI might be inhibiting  
452 superoxide accumulation in a different location. It will be important to determine the cellular  
453 location of both the superoxide accumulation and  $\text{Ca}^{2+}$  signal in the future.

454 Confirming the direct targets of these chemicals will be important to define these signalling  
455 pathways. A forward genetic approach lacks sufficient specificity and the likelihood of  
456 isolating loss-of-function mutations in essential sugar signalling proteins will be small, since  
457 these are expected to be lethal. Reverse genetics is limited when there is functional  
458 redundancy within protein families. Therefore, chemical proteomics has the most promise  
459 (Hicks & Raikhel, 2014), although these techniques can be particularly challenging for  
460 membrane proteins. Nevertheless, this chemical screen has successfully identified a new set  
461 of potential tools to manipulate sugar signalling in plant cells. This provides opportunity to  
462 discover new signalling pathways in *Arabidopsis* and it will be informative to test the  
463 efficacy of these chemicals in other plant species.

#### 464 **Acknowledgements**

465 We thank Waheed Arshad and Heather Eastmond for technical assistance and Heather  
466 McFarlane and Antony Dodd for sharing seed. This research was funded by a Royal Society  
467 Research Grant (RG150144), the Botany Foundation and the University of Melbourne  
468 through the Research Grants Support Scheme to MJH and Melbourne Research Scholarships  
469 to XL and GC.

#### 470 **Author Contribution**

471 MJH conceived the study; all authors designed experiments and analysed data; XL, DD, GC,  
472 AR, CCMB and MJH performed experiments; XL and MJH wrote the manuscript; all authors  
473 edited and approved the manuscript.

474 **Data Availability**

475 Raw sequencing files and processed data for RNA-seq have been deposited in the NCBI  
476 Gene Expression Omnibus [GSE188596].

477 **References**

478 **Baena-González E, Rolland F, Thevelein JM, Sheen J. 2007.** A central integrator of transcription  
479 networks in plant stress and energy signalling. *Nature* **448**: 938–942.

480 **Belda-Palazón B, Adamo M, Valerio C, Ferreira LJ, Confraria A, Reis-Barata D, Rodrigues A,  
481 Meyer C, Rodriguez PL, Baena-González E. 2020.** A dual function of SnRK2 kinases in the  
482 regulation of SnRK1 and plant growth. *Nature Plants* **6**.

483 **Burkart GM, Brandizzi F. 2021.** A Tour of TOR Complex Signaling in Plants. *Trends in  
484 Biochemical Sciences* **46**: 417–428.

485 **Cao P, Kim SJ, Xing A, Schenck CA, Liu L, Jiang N, Wang J, Last RL, Brandizzi F. 2019.**  
486 Homeostasis of branched-chain amino acids is critical for the activity of TOR signaling in  
487 *Arabidopsis*. *eLife* **8**.

488 **Chen Y, Chen Y, Shi C, Huang Z, Zhang Y, Li S, Li Y, Ye J, Yu C, Li Z, et al. 2018.** SOAPnuke:  
489 A MapReduce acceleration-supported software for integrated quality control and preprocessing of  
490 high-throughput sequencing data. *GigaScience* **7**: 1–6.

491 **Chen Y, Ji F, Xie H, Liang J, Zhang J. 2006.** The regulator of G-protein signaling proteins involved  
492 in sugar and abscisic acid signaling in *Arabidopsis* seed germination. *Plant Physiology* **140**: 302–310.

493 **Chen J-G, Willard FS, Huang J, Liang J, Chasse S a, Jones AM, Siderovski DP. 2003.** A seven-  
494 transmembrane RGS protein that modulates plant cell proliferation. *Science (New York, N.Y.)* **301**:  
495 1728–1731.

496 **Chen Q, Xu X, Xu D, Zhang H, Zhang C, Li G. 2019.** WRKY18 and WRKY53 coordinate with  
497 HISTONE ACETYLTRANSFERASE1 to regulate rapid responses to sugar. *Plant Physiology* **180**:  
498 2212–2226.

499 **Cho YH, Yoo SD, Sheen J. 2006.** Regulatory Functions of Nuclear Hexokinase1 Complex in  
500 Glucose Signaling. *Cell* **127**: 579–589.

501 **Cuadros-Inostroza Á, Caldana C, Redestig H, Kusano M, Lisec J, Peña-Cortés H, Willmitzer L, Hannah MA. 2009.** TargetSearch - a Bioconductor package for the efficient preprocessing of GC-MS  
502 metabolite profiling data. *BMC Bioinformatics* **10**.

503  
504 **Dalchau N, Baek SJ, Briggs HM, Robertson FC, Dodd AN, Gardner MJ, Stancombe M a, Haydon MJ, Stan G-B, Gonçalves JM, et al. 2011.** The circadian oscillator gene GIGANTEA  
505 mediates a long-term response of the *Arabidopsis thaliana* circadian clock to sucrose. *Proceedings of  
506 the National Academy of Sciences of the United States of America* **108**: 5104–5109.

507  
508 **Dalchau N, Hubbard KE, Robertson FC, Hotta CT, Briggs HM, Stan G-B, Gonçalves JM, Webb A a R. 2010.** Correct biological timing in *Arabidopsis* requires multiple light-signaling  
509 pathways. *Proceedings of the National Academy of Sciences of the United States of America* **107**:  
510 13171–13176.

511  
512 **Demidchik V. 2018.** ROS-activated ion channels in plants: Biophysical characteristics, physiological  
513 functions and molecular nature. *International Journal of Molecular Sciences* **19**.

514  
515 **Doyle MR, Davis SJ, Bastow RM, McWatters HG, Kozma-Bognár L, Nagy F, Millar AJ, Amasino RM. 2002.** The ELF4 gene controls circadian rhythms and flowering time in *Arabidopsis*  
516 *thaliana*. *Nature* **419**: 74–77.

517  
518 **Eastmond PJ, van Dijken AJH, Spielman M, Kerr A, Tissier AF, Dickinson HG, Jones JDG, Smeekens SC, Graham I a. 2002.** Trehalose-6-phosphate synthase 1, which catalyses the first step in  
519 trehalose synthesis, is essential for *Arabidopsis* embryo maturation. *Plant Journal* **29**: 225–235.

520  
521 **Figueroa CM, Lunn JE. 2016.** A tale of two sugars: Trehalose 6-phosphate and sucrose. *Plant  
Physiology* **172**: 7–27.

522  
523 **Frank A, Matiolli CC, Viana JC, Vincentz M, Webb AAR, Dodd AN, Viana JC, Hearn TJ, Kusakina J. 2018.** Circadian entrainment in *Arabidopsis* by the sugar-responsive transcription factor  
524 bZIP63. *Current Biology* **28**: 2597–2606.

525  
526 **Fricker MD, Plieth C, Knight H, Blancaflor E, Knight MR, White NS, Gilroy S. 1999.** Fluorescence and luminescence techniques to probe ion activities in living plant cells. . In: Mason  
527 WT, ed. *Fluorescent and Luminescent Probes for Biological Activity : A Practical Guide to  
528 Technology for Quantitative Real-Time Analysis*. Elsevier, 569–596.

529 **Ganpudi A, Romanowski A, Halliday KJ. 2019.** HEXOKINASE 1 Glycolytic Action Fuels Post-  
530 Germinative Seedling Growth. *bioRxiv*.

531 **Giavalisco P, Li Y, Matthes A, Eckhardt A, Hubberten HM, Hesse H, Segu S, Hummel J, Köhl  
532 K, Willmitzer L. 2011.** Elemental formula annotation of polar and lipophilic metabolites using  $^{13}\text{C}$ ,  
533  $^{15}\text{N}$  and  $^{34}\text{S}$  isotope labelling, in combination with high-resolution mass spectrometry. *Plant Journal*  
534 **68:** 364–376.

535 **Gómez LD, Gilday A, Feil R, Lunn JE, Graham IA. 2010.** AtTPS1-mediated trehalose 6-phosphate  
536 synthesis is essential for embryogenic and vegetative growth and responsiveness to ABA in  
537 germinating seeds and stomatal guard cells. *Plant Journal* **64:** 1–13.

538 **Haydon MJ, Kawachi M, Wirtz M, Hillmer S, Hell R, Krämer U. 2012.** Vacuolar nicotianamine  
539 has critical and distinct roles under iron deficiency and for zinc sequestration in *Arabidopsis*. *The  
540 Plant cell* **24:** 724–37.

541 **Haydon MJ, Mielczarek O, Frank A, Román Á, Webb AAR. 2017.** Sucrose and ethylene signaling  
542 interact to modulate the circadian clock. *Plant Physiology* **175:** 947–958.

543 **Haydon MJ, Mielczarek O, Robertson FC, Hubbard KE, Webb AAR. 2013.** Photosynthetic  
544 entrainment of the *Arabidopsis thaliana* circadian clock. *Nature* **502:** 689–92.

545 **Hicks GR, Raikhel N v. 2014.** Plant chemical biology: Are we meeting the promise? *Frontiers in  
546 Plant Science* **5**.

547 **Huang JP, Tunc-Ozdemir M, Chang Y, Jones AM. 2015.** Cooperative control between AtRGS1  
548 and AtHXR1 in a WD40-repeat protein pathway in *Arabidopsis thaliana*. *Frontiers in Plant Science*  
549 **6**.

550 **Huege J, Krall L, Steinhauser MC, Giavalisco P, Rippka R, Tandeau De Marsac N, Steinhauser  
551 D. 2011.** Sample amount alternatives for data adjustment in comparative cyanobacterial  
552 metabolomics. *Analytical and Bioanalytical Chemistry* **399:** 3503–3517.

553 **Jones AM, Ecker JR, Chen JG. 2003.** A reevaluation of the role of the heterotrimeric G protein in  
554 coupling light responses in *arabidopsis*. *Plant Physiology* **131:** 1623–1627.

555 **Kim D, Langmead B, Salzberg SL. 2015.** HISAT: A fast spliced aligner with low memory  
556 requirements. *Nature Methods* **12:** 357–360.

557 **Kong D, Hu H-C, Okuma E, Lee Y, Lee HS, Munemasa S, Cho D, Ju C, Pedoeim L, Rodrigues  
558 B, et al. 2016.** L-Met Activates *Arabidopsis* GLR Ca  $2+$  Channels Upstream of ROS Production and

559 Regulates Stomatal Report L-Met Activates Arabidopsis GLR Ca 2 + Channels Upstream of ROS  
560 Production and Regulates Stomatal Movement. *Cell Reports* **17**: 2553–2561.

561 **Li B, Dewey CN. 2011.** RSEM: Accurate transcript quantification from RNA-Seq data with or  
562 without a reference genome. *BMC Bioinformatics* **12**.

563 **List M, Schmidt S, Christiansen H, Rehmsmeier M, Tan Q, Mollenhauer J, Baumbach J. 2016.**  
564 Comprehensive analysis of high-throughput screens with HiTSeekR. *Nucleic Acids Research* **44**:  
565 6639–6648.

566 **Liu W, Feke A, Leung CC, Tarté DA, Yuan W, Vanderwall M, Sager G, Wu X, Schear A, Clark  
567 DA, et al. 2021.** A metabolic daylength measurement system mediates winter photoperiodism in  
568 plants. *Developmental Cell* **56**: 2501-2515.e5.

569 **Mair A, Pedrotti L, Wurzinger B, Anrather D, Simeunovic A, Weiste C, Valerio C, Dietrich K,  
570 Kirchler T, Nägele T, et al. 2015.** SnRK1-triggered switch of bZIP63 dimerization mediates the low-  
571 energy response in plants. *eLife* **4**: 1–33.

572 **Menand B, Desnos T, Nussaume L, Berger F, Bouchez D, Meyer C, Robaglia C. 2002.**  
573 Expression and disruption of the Arabidopsis TOR (target of rapamycin) gene. *Proceedings of the  
574 National Academy of Sciences of the United States of America* **99**: 6422–6427.

575 **Montané MH, Menand B. 2013.** ATP-competitive mTOR kinase inhibitors delay plant growth by  
576 triggering early differentiation of meristematic cells but no developmental patterning change. *Journal  
577 of Experimental Botany* **64**: 4361–4374.

578 **Moore B, Zhou L, Rolland F, Hall Q, Cheng W-H, Liu Y-X, Hwang I, Jones T, Sheen J. 2003.**  
579 Role of the Arabidopsis Glucose Sensor HXK1 in Nutrient, Light, and Hormonal Signaling. *Science*  
580 **300**: 332–336.

581 **Nakamichi N, Kita M, Ito S, Yamashino T, Mizuno T. 2005.** PSEUDO-RESPONSE  
582 REGULATORS, PRR9, PRR7 and PRR5, Together play essential roles close to the circadian clock of  
583 Arabidopsis thaliana. *Plant and Cell Physiology* **46**: 686–698.

584 **Peixoto B, Moraes TA, Mengin V, Margalha L, Vicente R, Feil R, Höhne M, Sousa AGG, Lilue  
585 J, Stitt M, et al. 2021.** Impact of the SnRK1 protein kinase on sucrose homeostasis and the  
586 transcriptome during the diel cycle. *Plant Physiology*.

587 **Porra RJ. 1989.** Determination of accurate extinction coefficients and simultaneous equations for  
588 assaying chlorophylls a and b extracted with four different solvents : verification of the concentration  
589 of chlorophyll standards by atomic absorption spectroscopy. **975**: 384–394.

590 **Portolés S, Más P. 2010.** The functional interplay between protein kinase CK2 and cca1  
591 transcriptional activity is essential for clock temperature compensation in *Arabidopsis*. *PLoS Genetics*  
592 **6**: e1001201.

593 **Ramon M, Dang TTV, Broeckx T, Hulsmans S, Crepin N, Sheen J, Rolland F. 2019.** Default  
594 activation and nuclear translocation of the plant cellular energy sensor SnRK1 regulate metabolic  
595 stress responses and development. *Plant Cell* **31**: 1614–1632.

596 **Roessner U, Luedemann A, Brust D, Fiehn O, Linke T, Willmitzer L, Fernie AR. 2001.**  
597 *Metabolic Profiling Allows Comprehensive Phenotyping of Genetically or Environmentally Modified*  
598 *Plant Systems*.

599 **Rolland F, Baena-Gonzalez E, Sheen J. 2006.** Sugar sensing and signaling in plants: conserved and  
600 novel mechanisms. *Annual review of plant biology* **57**: 675–709.

601 **Román Á, Li X, Deng D, Davey JW, James S, Graham IA, Haydon MJ. 2021.** Superoxide is  
602 promoted by sucrose and affects amplitude of circadian rhythms in the evening. *Proceedings of the*  
603 *National Academy of Sciences of the United States of America* **118**.

604 **Ruijter JM, Ramakers C, Hoogaars WMH, Karlen Y, Bakker O, van den hoff MJB, Moorman**  
605 **AFM. 2009.** Amplification efficiency: Linking baseline and bias in the analysis of quantitative PCR  
606 data. *Nucleic Acids Research* **37**.

607 **Stacklies W, Redestig H, Scholz M, Walther D, Selbig J. 2007.** pcaMethods - A bioconductor  
608 package providing PCA methods for incomplete data. *Bioinformatics* **23**: 1164–1167.

609 **Sun Y, Qiao Z, Muchero W, Chen J-G. 2020.** Lectin Receptor-Like Kinases: The Sensor and  
610 Mediator at the Plant Cell Surface. *Frontiers in Plant Science* **11**.

611 **Tarazona S, Furió-Tarí P, Turrà D, di Pietro A, Nueda MJ, Ferrer A, Conesa A. 2015.** Data  
612 quality aware analysis of differential expression in RNA-seq with NOISeq R/Bioc package. *Nucleic*  
613 *Acids Research* **43**.

614 **Thorne N, Shen M, Lea WA, Simeonov A, Lovell S, Auld DS, Inglese J. 2012.** Firefly luciferase in  
615 chemical biology: A compendium of inhibitors, mechanistic evaluation of chemotypes, and suggested  
616 use as a reporter. *Chemistry and Biology* **19**: 1060–1072.

617 **Thung L, Trusov Y, Chakravorty D, Botella JR. 2012.**  $G\gamma 1+G\gamma 2+G\gamma 3=G\beta$ : The search for  
618 heterotrimeric G-protein  $\gamma$  subunits in Arabidopsis is over. *Journal of Plant Physiology* **169**: 542–545.

619 **Ting MKY, Zoschke R, Haydon Michael J. 2022.** Agrobacterium-mediated seedling transformation  
620 to measure circadian rhythms in Arabidopsis. In: Staiger D, Davis SJ, Davis AM, eds. *Plant Circadian*  
621 *Networks: Methods and Protocols*. New York: Springer, 57–64.

622 **Ullah H, Chen J, Temple B, Boyes DC, Alonso JM, Davis KR, Ecker JR, Jones AM. 2003.** The  $\beta$ -  
623 Subunit of the Arabidopsis G Protein Negatively Regulates Auxin-Induced Cell Division and Affects  
624 Multiple Developmental Processes. **15**: 393–409.

625 **Urano D, Phan N, Jones JC, Yang J, Huang J, Grigston J, Taylor JP, Jones AM. 2012.**  
626 Endocytosis of the seven-transmembrane RGS1 protein activates G-protein-coupled signalling in  
627 Arabidopsis. *Nature Cell Biology* **14**: 1079–1088.

628 **Wang Y, Chang H, Hu S, Lu X, Yuan C, Zhang C, Wang P, Xiao W, Xiao L, Xue G, et al. 2014.**  
629 Plastid casein kinase 2 knockout reduces abscisic acid (ABA) sensitivity, thermotolerance, and  
630 expression of ABA- and heat-stress-responsive nuclear genes. **65**: 4159–4175.

631 **Weckwerth W, Ehlers Loureiro M, Wenzel K, Fiehn O. 2004.** *Differential metabolic networks*  
632 *unravel the effects of silent plant phenotypes*.

633 **Xiong Y, McCormack M, Li L, Hall Q, Xiang C, Sheen J. 2013.** Glucose-TOR signalling  
634 reprograms the transcriptome and activates meristems. *Nature* **496**: 181–6.

635 **Zhang N, Meng Y, Li X, Zhou Y, Ma L, Fu L, Schwarzländer M, Liu H, Xiong Y. 2019.**  
636 Metabolite-mediated TOR signaling regulates the circadian clock in Arabidopsis. *Proceedings of the*  
637 *National Academy of Sciences of the United States of America* **116**: 25395–25397.

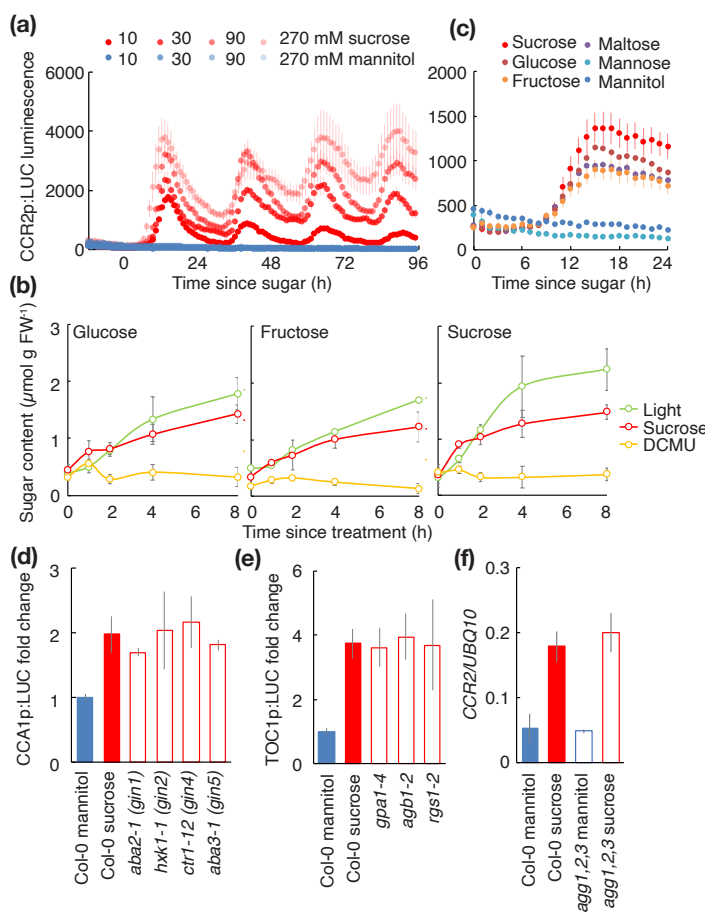
638 **Zhang Y, Primavesi LF, Jhurreea D, Andralojc PJ, Mitchell R a C, Powers SJ, Schluepmann H,**  
639 **Delatte T, Wingler A, Paul MJ. 2009.** Inhibition of SNF1-related protein kinase1 activity and  
640 regulation of metabolic pathways by trehalose-6-phosphate. *Plant physiology* **149**: 1860–71.

641

642

643

644



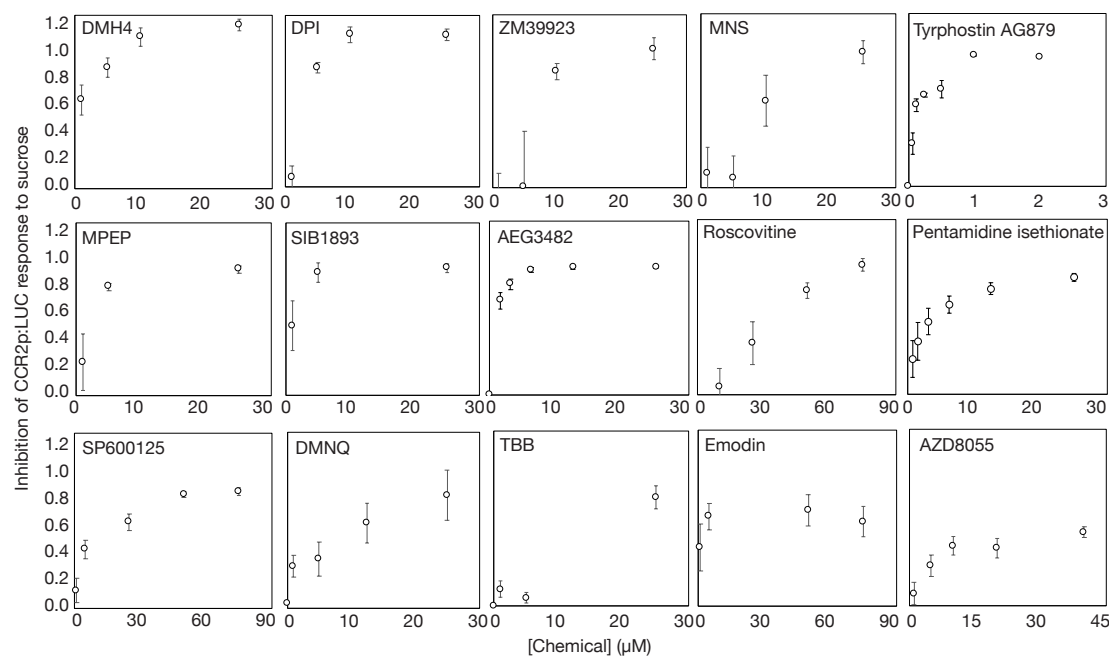
645

646 Figure 1. A sugar response assay in Arabidopsis seedlings. (a) Luciferase luminescence in  
 647 dark-adapted *CCR2p:LUC* seedlings treated with indicated concentration of sucrose or  
 648 mannitol (means  $\pm$  SEM,  $n = 6$ ). (b) Sugar content in dark-adapted seedlings treated with 30  
 649 mM sucrose or transferred into the light with or without DCMU (means  $\pm$  SD,  $n = 4$ ). (c)  
 650 Luciferase luminescence in dark-adapted *CCR2p:LUC* seedlings treated with 30 mM sugars  
 651 (means  $\pm$  SEM,  $n = 8$ ). (d) and (e) Fold change in luciferase reporter luminescence in dark-  
 652 adapted wild-type (Col-0) or mutant seedlings treated with mannitol (blue) or sucrose (red)  
 653 (means  $\pm$  SD,  $n = 4$ ). (f) *CCR2* transcript level, normalised to *UBQ10*, in dark-adapted wild-  
 654 type (Col-0) or *agg1 agg2 agg3* mutant seedlings 12 h after treatment with mannitol (blue) or  
 655 sucrose (red) (means  $\pm$  SD,  $n = 3$ ).

656

657

658



659

660

661

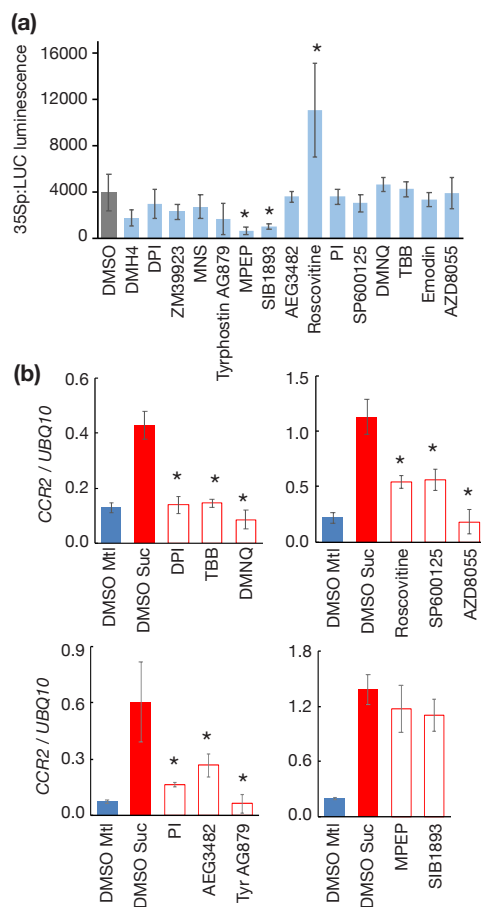
662 Figure 2. Dose response of transcriptional response to sucrose for 15 chemicals. Inhibition of  
663 peak luciferase luminescence in dark-adapted *CCR2p:LUC* seedlings after treatment with 30  
664 mM sucrose in the presence of the indicated concentration of chemical (means ± SD, n = 6-  
665 12).

666

667

668

669



670

671

672

673 Figure 3. Validation of transcriptional effect of LOPAC chemicals. (a) Luciferase  
674 luminescence in *35Sp:LUC* seedlings, 16 h after transfer to media containing the minimum  
675 effective concentration of each chemical (means  $\pm$  SD, n = 8; \* p > 0.05, Bonferroni-  
676 corrected *t*-test) (b) *CCR2* transcript level, relative to *UBQ10*, in dark-adapted Col-0  
677 seedlings 12 h after treatment with 30 mM mannitol (blue), 30 mM sucrose (red) or 30 mM  
678 sucrose in the presence of the minimum effective concentration of chemical (white) (means  $\pm$   
679 SD, n = 4; \* p > 0.05, Bonferroni-corrected *t*-test).

680

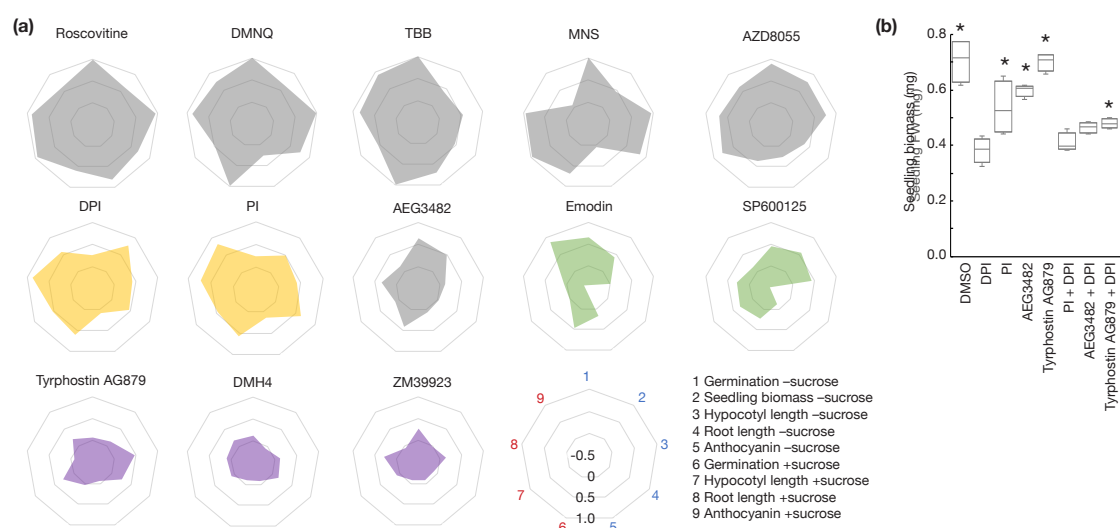
681

682

683

684

685



686

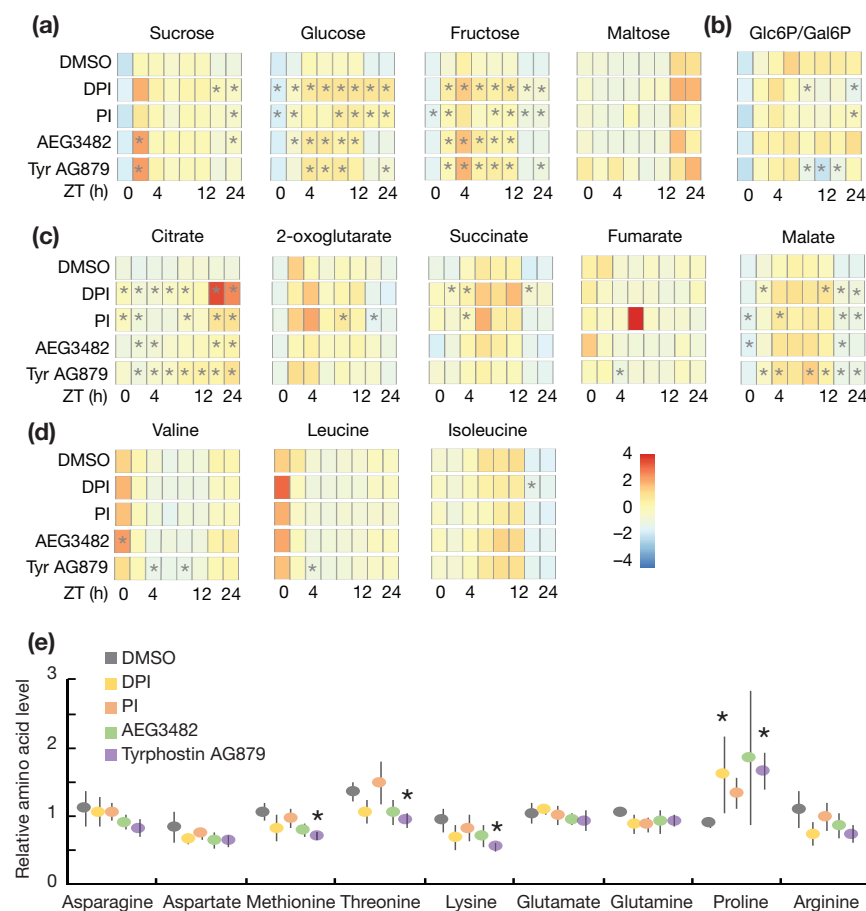
687

688 Figure 4. Summary of effects of LOPAC chemicals on sugar-related growth phenotypes. (a)  
689 Normalised effects of minimum effective concentration of 13 LOPAC chemicals on  
690 germination of dormant seeds on 30 mM mannitol (1) or sucrose (6), biomass of 7 d old  
691 seedlings on 1/2 MS (2), hypocotyl and root length of 7 d old dark-grown seedlings on 30 mM  
692 mannitol (3,4) or sucrose (7,8) and anthocyanin content in 9 d old seedlings grown for 2 d on  
693 90 mM mannitol (5) or sucrose (9). Complete data are shown in Fig S4 and Fig S5. (b)  
694 Seedling biomass of 7 d old seedlings sown on 1/2 MS containing DMSO, 2 μM DPI, 5 μM  
695 PI, 2.5 μM AEG3482 or 0.5 μM Tyrphostin AG879 alone or in combination (n = 4 of 12  
696 seedlings; \* p < 0.05 compared to DPI, Bonferroni-corrected *t*-test).

697

698

699



700

701

702

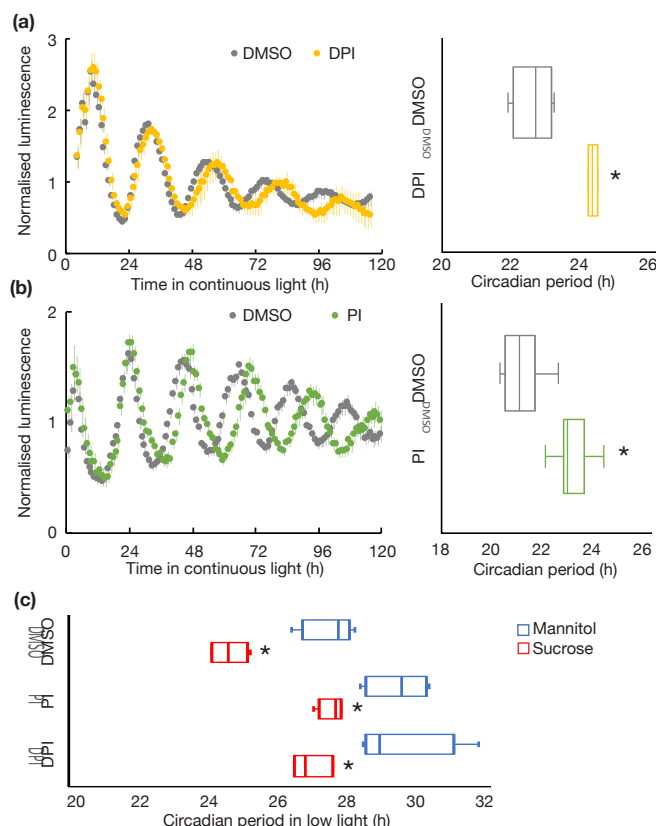
703 Figure 5. Primary metabolite levels in chemical-treated seedlings. (a-d) Heatmaps of relative  
 704 metabolite levels in seedlings treated with DMSO or chemicals at ZT23 and sampled at ZT0,  
 705 ZT1.5, ZT4, ZT8, ZT10.5, ZT12, ZT22.5 and ZT24 ( $n = 5$ ; \*  $p < 0.05$  compared to DMSO,  $t$ -  
 706 test). (e) Relative amino acid levels in DMSO- or chemical-treated seedlings at ZT10.5 (mean  
 707  $\pm$  SD,  $n = 5$ ; \*  $p < 0.01$  compared to DMSO,  $t$ -test).

708

709

710

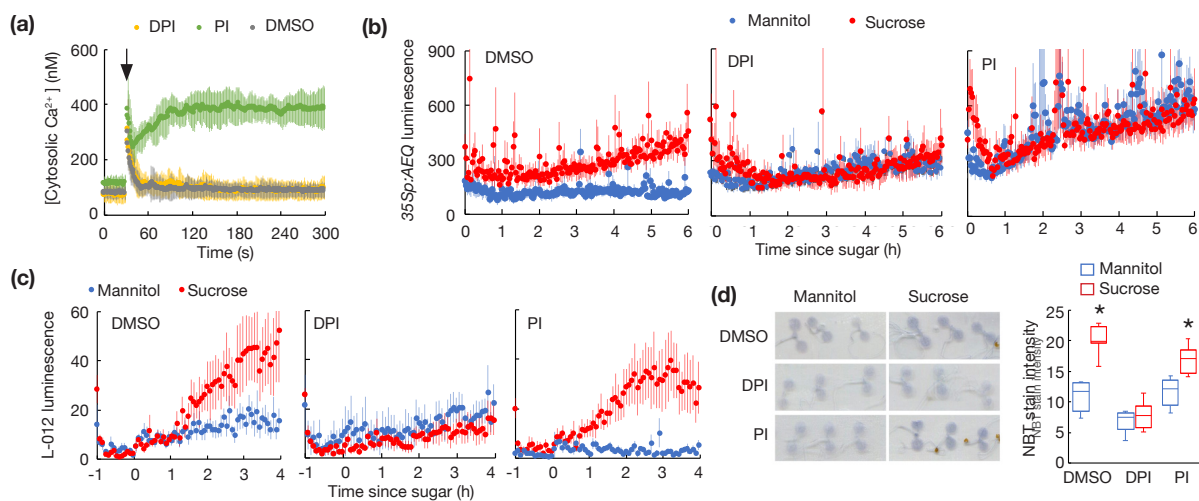
711



712

713 Figure 6. Effect of PI and DPI on circadian period. Normalised luciferase luminescence and  
714 circadian period estimates in (a) *TOC1p:LUC* (n = 4) or (b) *CCA1p:LUC* seedlings (n = 16)  
715 treated with DMSO, 10  $\mu$ M DPI or 25  $\mu$ M PI before transfer to continuous light (n = 4; \* p <  
716 0.05, Student's t-test). (c) Circadian period estimates of *CCA1p:LUC* seedlings treated with  
717 DMSO, 10  $\mu$ M DPI or 25  $\mu$ M PI with 30 mM mannitol or sucrose before transfer into  
718 continuous low light (n = 4; \* p < 0.05 compared to mannitol, Bonferroni-corrected t-test).

719



720

721

722 Figure 7. Effect of PI on elevation of cytosolic  $\text{Ca}^{2+}$  by sucrose. (a) Cytosolic  $\text{Ca}^{2+}$   
723 concentration in  $35\text{Sp:AEQ}$  seedlings treated (arrow) with DMSO (control), 10  $\mu\text{M}$  DPI or 25  
724  $\mu\text{M}$  PI (means  $\pm$  SD,  $n = 6$ ). (b) Aequorin luminescence in dark-adapted  $35\text{Sp:AEQ}$  seedlings  
725 treated with 30 mM sucrose or mannitol in the presence of DMSO, 5  $\mu\text{M}$  DPI or 25  $\mu\text{M}$  PI  
726 (mean  $\pm$  SD,  $n = 6$ ). (c) L-012 luminescence in dark-adapted Col-0 seedlings treated with 30  
727 mM mannitol or sucrose in the presence of DMSO, 10  $\mu\text{M}$  DPI or 25  $\mu\text{M}$  PI (means  $\pm$  SEM,  
728  $n = 6$ ). (d) Images and quantification of nitroblue tetrazolium (NBT) stain for superoxide in  
729 dark-adapted Col-0 seedlings 4 h after treatment with 30 mM mannitol or sucrose in the  
730 presence of DMSO, 5  $\mu\text{M}$  DPI or 25  $\mu\text{M}$  PI ( $n = 8$ ; \*  $p < 0.05$  compared to mannitol,  
731 Bonferroni-corrected  $t$ -test).

732

733

734

735

736

737

738 **Table 1. Chemical modifiers of *CCR2p:LUC* response to sucrose**

| Chemical Name   | PubChem_CID | rzscore | SSMD  | Primary mammalian target                                      |
|---|-------------|---------|-------|---|
| Tyrphostin AG 879   | 135419190   | -13.88  | -5.87 | TrkA, tyrosine kinase   |
| 3,3'-Difluorobenzaldazine (DFB)                             | 006604893   | -3.99   | -5.13 | mGluR5, metabotropic glutamate receptor                       |
| 6-Methyl-2-(phenylethynyl)pyridine hydrochloride (MPEP) * ‡ | 009794588   | -6.58   | -4.88 | mGluR5, metabotropic glutamate receptor                       |
| 5-Nitro-2-(3-phenylpropylamino)benzoic acid (NPPB)          | 000004549   | -1.80   | -4.84 | Cl <sup>-</sup> channel                                       |
| 1,9-Pyrazolanthrone (SP600125)                              | 000008515   | -3.81   | -4.83 | c-Jun N-terminal kinase (c-JNK), MAP kinase                   |
| 2-methyl-6-(2-Phenylethenyl)Pyridine (SIB 1893)             | 005311432   | -6.32   | -4.60 | mGluR5, metabotropic glutamate receptor                       |
| MTEP hydrochloride  | 045073467   | -5.07   | -3.78 | mGluR5, metabotropic glutamate receptor                       |
| L2-b  | 039247144   | -5.59   | -3.74 | Amyloid- $\beta$  |
| Riluzole  | 000005070   | -4.10   | -3.56 | Na <sup>+</sup> channel                                       |
| AEG 3482  | 000698112   | -4.86   | -3.39 | Heat shock protein 90 (HSP90)                                 |
| Niclosamide   | 000004477   | -2.70   | -3.30 | Oxidative phosphorylation                                     |
| CGP-7930  | 005024764   | -4.03   | -3.26 | GABA-B receptor, GPCR   |
| Tyrphostin 51   | 005328807   | -2.26   | -3.22 | EGF receptor, tyrosine kinase                                 |
| 4,5,6,7-Tetrabromobenzotriazole (TBB)                       | 000001694   | -9.98   | -3.19 | Casein kinase 2 (CK2)   |
| Fenobam   | 000162834   | -1.32   | -3.12 | mGluR5, metabotropic glutamate receptor                       |
| DMH4  | 005329447   | -3.69   | -3.00 | VEGF receptor, tyrosine kinase                                |
| Bay 11-7082   | 005353431   | -2.07   | -2.81 | Nuclear factor-kappa B (NF- $\kappa$ B), transcription factor |
| 1-Phenyl-3-(2-thiazolyl)-2-thiourea ‡                       | 000719408   | -5.59   | -2.81 | Dopamine beta-hydroxylase                                     |
| BF-170 hydrochloride *                                      | 000297284   | -4.93   | -2.78 | Tau   |

|   |           |        |       |   |
|---|-----------|--------|-------|---|
| Diphenyleneiodonium chloride (DPI)        | 002733504 | -11.81 | -2.65 | Nitric oxide synthase (NOS)                       |
| CBIQ                                      | 011401613 | -2.18  | -2.65 | CFTR Cl <sup>-</sup> channel                      |
| PD 98,059 *                               | 000004713 | -4.29  | -2.58 | MAP kinase kinase (MAPKK)                         |
| Oltipraz metabolite M2                    | 000128585 | -4.38  | -2.57 | Liver X receptor alpha (LXR-alpha)                |
| Nocodazole *                              | 000004122 | -2.06  | -2.52 | Beta-tubulin                                      |
| L-165,041                                 | 006603901 | -3.39  | -2.44 | Peroxisome proliferator-activated receptor (PPAR) |
| Amlexanox * ‡                             | 000002161 | -5.63  | -2.37 | TANK-binding kinase 1, Ser/Thr kinase             |
| 2,3-Dimethoxy-1,4-naphthoquinone (DMNQ)   | 000003136 | -6.91  | -2.32 | Redox cycling agent                               |
| Rhodblock 6                               | 006466029 | -3.49  | -2.21 | Rho Kinase, Ser/Thr kinase                        |
| DCEBIO                                    | 000656765 | -1.48  | -2.20 | K <sup>+</sup> and Cl <sup>-</sup> channel        |
| 3,4,-Methylenedioxy-β-Nitrostyrene (MNS)  | 000672296 | -6.11  | -2.18 | Src and Syk tyrosine kinase                       |
| U0126                                     | 003006531 | -2.01  | -2.17 | MAP kinase kinase (MAPKK)                         |
| Gossypol                                  | 000003503 | -0.76  | -2.13 | Platelet activating factor (PAF)                  |
| SB-366791                                 | 000667594 | -2.73  | -2.12 | TRPV1 cation channel                              |
| L-alpha-Methyldopa                        | 000038853 | -0.55  | -2.02 | L-aromatic amino acid decarboxylase inhibitor     |
| SMER28                                    | 001560402 | -1.66  | -1.97 | Autophagy   |
| SIB 1757                                  | 006849066 | -3.69  | -1.92 | mGluR5, metabotropic glutamate receptor           |
| Sanguinarine chloride                     | 000068635 | -3.94  | -1.87 | Protein phosphatase 2C (PP2C)                     |
| Nimesulide                                | 000004495 | -3.16  | -1.81 | Cyclooxygenase-2 (COX-2)                          |
| Rabeprazole sodium                        | 014720269 | -1.62  | -1.75 | H <sup>+</sup> /K <sup>+</sup> ATPase             |
| ONO-RS-082 *                              | 006438389 | -0.90  | -1.61 | Phospholipase A2                                  |
| SU 4312                                   | 006450842 | -3.30  | -1.56 | VEGF receptor, tyrosine kinase                    |
| Diethylenetriaminepentaacetic acid (DTPA) | 000003053 | -1.02  | -1.55 | Metal chelator                                    |

|                                 |           |       |       |   |
|---------------------------------|-----------|-------|-------|---|
| JW55                            | 002946601 | -2.37 | -1.54 | Poly (ADP-ribose) polymerase (PARP)               |
| GBR-12909 dihydrochloride       | 000104920 | -3.43 | -1.52 | Dopamine reuptake                                 |
| AC-93253 iodide *               | 016078948 | -5.55 | -1.52 | Retinoic acid receptor (RARalpha)                 |
| Ro 61-8048                      | 005282337 | -2.16 | -1.51 | Kynureine 3 monooxygenase (KMO)                   |
| Flunarizine dihydrochloride     | 005282407 | -1.85 | -1.50 | Ca <sup>2+</sup> /Na <sup>+</sup> channel         |
| BIO                             | 005287844 | -0.95 | -1.49 | Glycogen synthase kinase 3 (GSK-3)                |
| Pentamidine isethionate         | 000008813 | -1.48 | -1.49 | NMDA glutamate receptor, Ca <sup>2+</sup> channel |
| ZM 39923 hydrochloride          | 000176406 | -3.70 | -1.46 | Janus kinase 3 (JNK-3), tyrosine kinase           |
| Diclofenac sodium               | 005018304 | -1.71 | -1.44 | Cyclooxygenase (COX)                              |
| Phosphonoacetic acid            | 000000546 | -0.88 | -1.42 | DNA polymerase                                    |
| Emodin                          | 000003220 | -1.57 | -1.37 | Casein kinase 2 (CK2)                             |
| PF 3845 hydrate                 | 025154867 | -2.32 | -1.37 | Fatty acid amide hydrolase (FAAH)                 |
| Naltrindole hydrochloride       | 016219715 | -0.37 | -1.35 | Delta opioid receptor, GPCR                       |
| Tranylcypromine hydrochloride   | 002723716 | -0.71 | -1.34 | Monoamine oxidase                                 |
| KRM-III                         | 000736689 | -2.41 | -1.34 | T cell antigen receptor (TCR)                     |
| 3,4-Dichloroisocoumarin         | 000001609 | -2.23 | -1.38 | Serine protease                                   |
| Reactive Blue 2                 | 000108094 | -1.54 | -1.32 | P2Y, purigenic GPCR                               |
| TBBz                            | 005149739 | -1.36 | -1.31 | Casein kinase 2 (CK2)                             |
| Nemadipine-A                    | 002856102 | -0.61 | -1.31 | L-type Ca <sup>2+</sup> channel                   |
| Danazol                         | 000028417 | -1.82 | -1.31 | Androgen receptor, transcription factor           |
| Nitisinone                      | 000115355 | -1.34 | -1.30 | 4-Hydroxyphenylpyruvate dioxygenase (HPPD)        |
| Leflunomide                     | 000003899 | -1.35 | -1.28 | Dihydroorotate dehydrogenase                      |
| 6(5H)-Phenanthridinone          | 000001853 | -1.82 | -1.28 | Poly (ADP-ribose) polymerase (PARP)               |
| 5alpha-Pregnan-3alpha-ol-20-one | 000092786 | 1.24  | 1.31  | GABA-A receptor, ion channel                      |

|                                   |           |      |      |   |
|-----------------------------------|-----------|------|------|---|
| A3 hydrochloride                  | 009861903 | 1.03 | 1.34 | Casein kinase (CK)                            |
| Candesartan cilexetil             | 000002540 | 0.99 | 1.39 | Angiotensin II receptor (ATR), GPCR           |
| S-Methyl-L-thiocitrulline acetate | 011957614 | 0.99 | 1.41 | Nitric oxide synthase (NOS)                   |
| Methoxamine hydrochloride         | 000006081 | 0.81 | 1.41 | Alpha1 adrenergic receptor, GPCR              |
| Piribedil maleate                 | 011957664 | 0.90 | 1.48 | Dopamine receptor, GPCR                       |
| Phentolamine mesylate             | 000091430 | 1.40 | 1.62 | Alpha adrenergic receptor, GPCR               |
| 1-Methylhistamine dihydrochloride | 011957601 | 0.86 | 1.64 | Histamine metabolite                          |
| Isonipecotic acid                 | 000003773 | 2.09 | 1.73 | GABA-A receptor, ion channel                  |
| GANT61                            | 000421610 | 1.07 | 1.75 | Zinc finger protein GLI, transcription factor |

739 \* Inhibited 35Sp:LUC

740 ‡ luciferase inhibitor from Thorne et al 2012

741

742

743

744

745

746

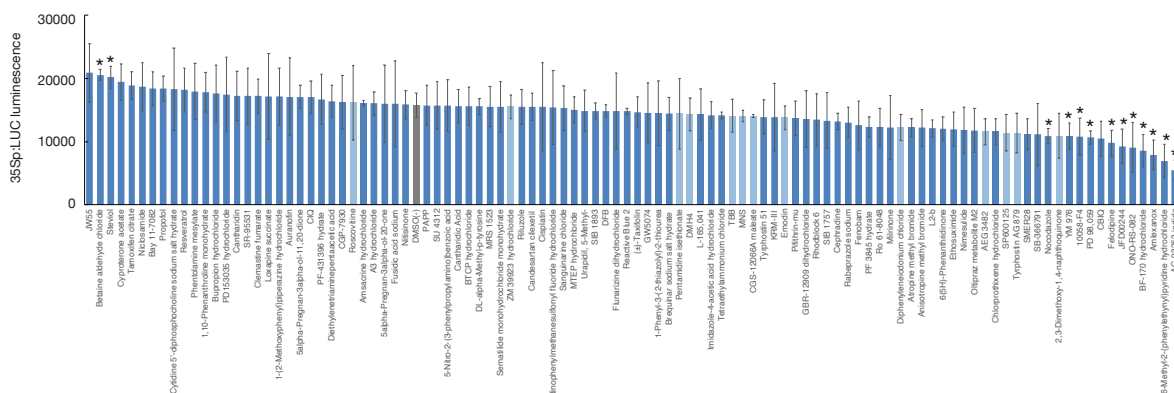
747

748

749

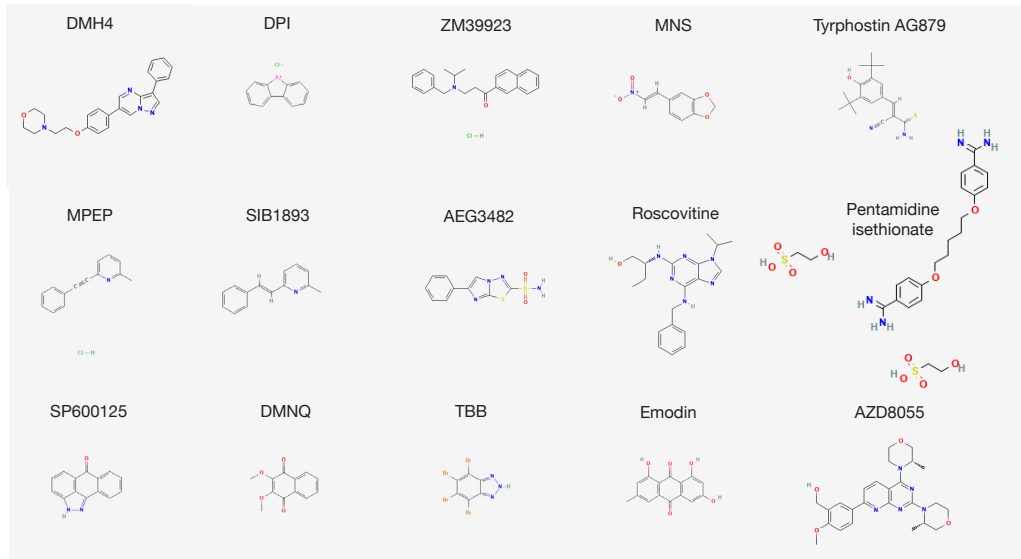
750

751



752

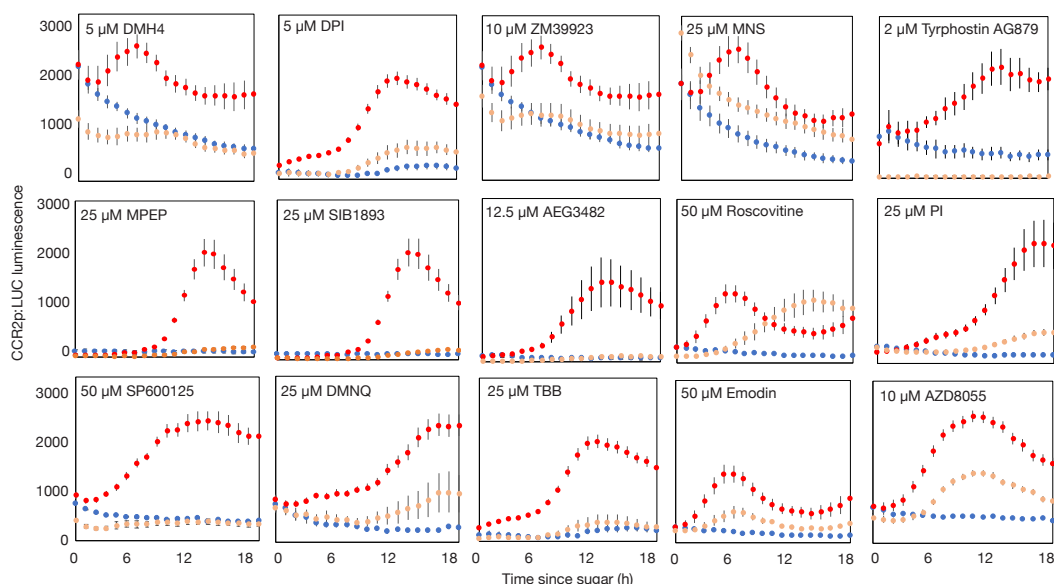
753 Figure S1. Inhibition of luciferase luminescence by LOPAC chemicals. Luciferase  
754 luminescence in *35Sp:LUC* seedlings, 6 h after transfer to media with 25  $\mu$ M chemical  
755 (means  $\pm$  SD, n = 3).



756

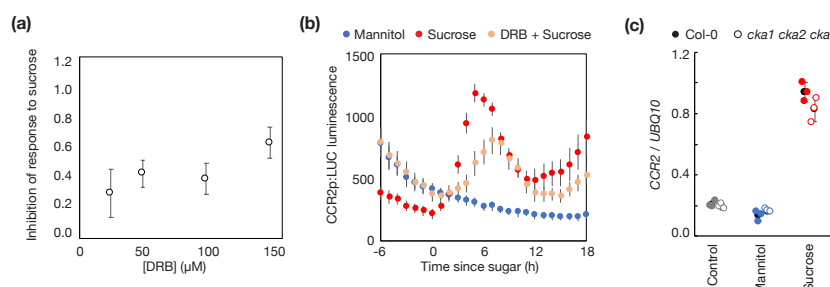
757 Figure S2. Structures of 15 chemicals chosen for validation. Chemical structures were  
758 obtained from Pubchem (<https://pubchem.ncbi.nlm.nih.gov>) and scaled to equivalent size.

759



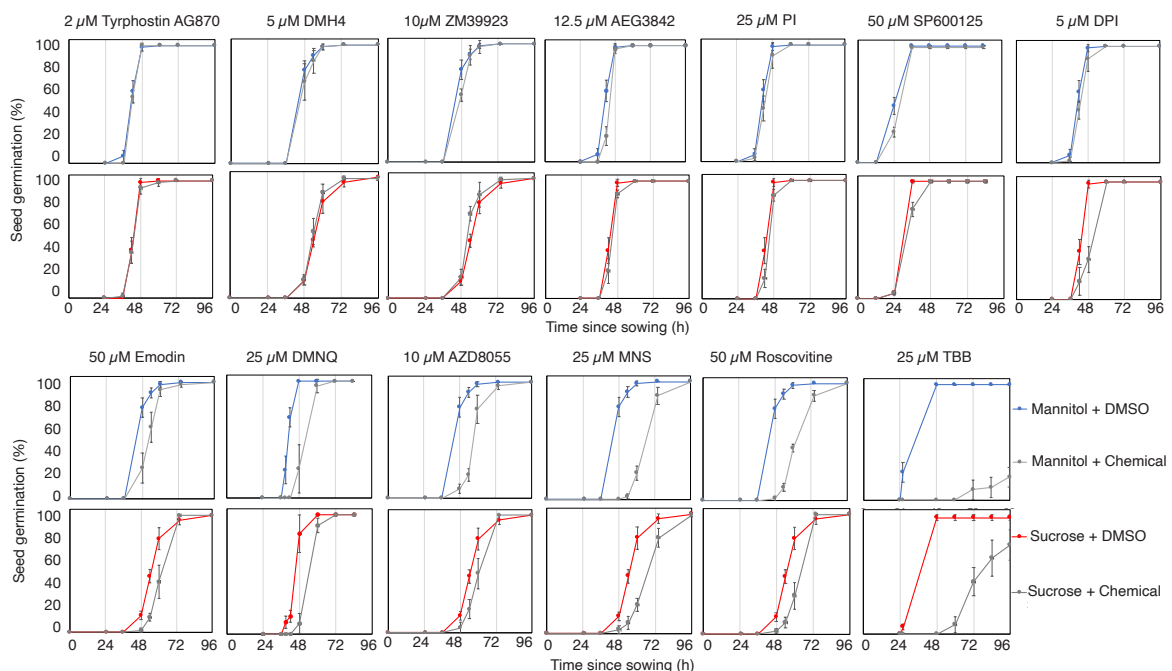
760

761 Figure S3. Inhibition of transcriptional response to sucrose. Luciferase luminescence in dark-  
762 adapted *CCR2p:LUC* seedlings following treatment with 30 mM mannitol (blue), 30 mM  
763 sucrose (red) or 30 mM sucrose and the indicated concentration of chemical (pink) (means  $\pm$   
764 SEM,  $n = 6-12$ ).



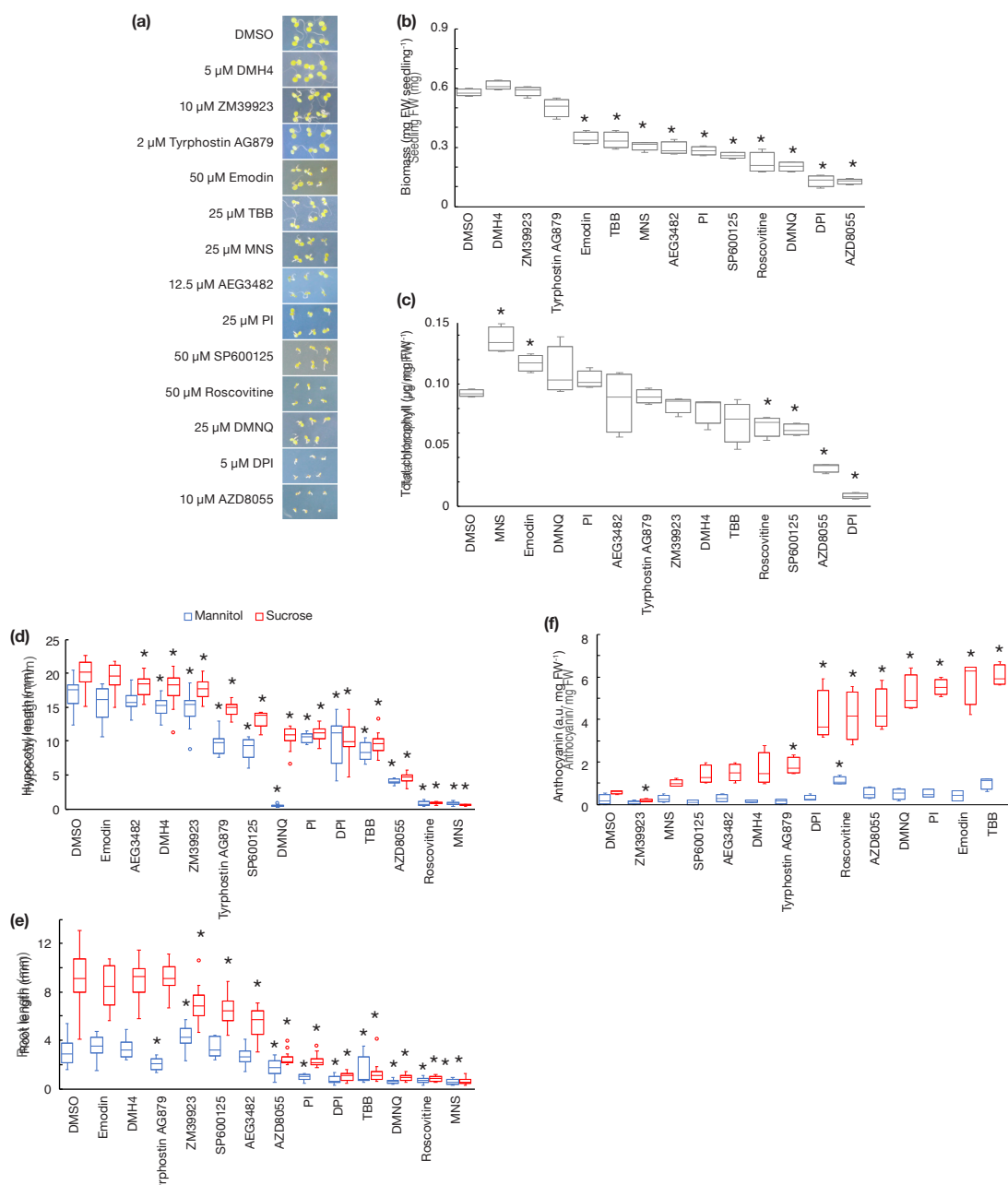
765

766 Figure S4. CK2 is not required for *CCR2* response to sucrose. (a) Inhibition of peak  
767 luciferase luminescence in dark-adapted *CCR2p:LUC* seedlings after treatment with 30 mM  
768 sucrose in the presence of the indicated concentration of DRB (means  $\pm$  SD,  $n = 8$ ). (b)  
769 Luciferase luminescence in dark-adapted *CCR2p:LUC* seedlings after treatment with 30 mM  
770 sucrose in the presence of 150  $\mu$ M DRB (means  $\pm$  SD,  $n = 8$ ). (c) *CCR2* transcript level,  
771 relative to *UBQ10*, in dark-adapted wild-type (Col-0) and *cka1-1 cka2-1 cka3-1* seedlings  
772 before (Control) or 12 h after treatment with 30 mM mannitol or 30 mM sucrose (means  $\pm$   
773 SD,  $n = 3$ ).



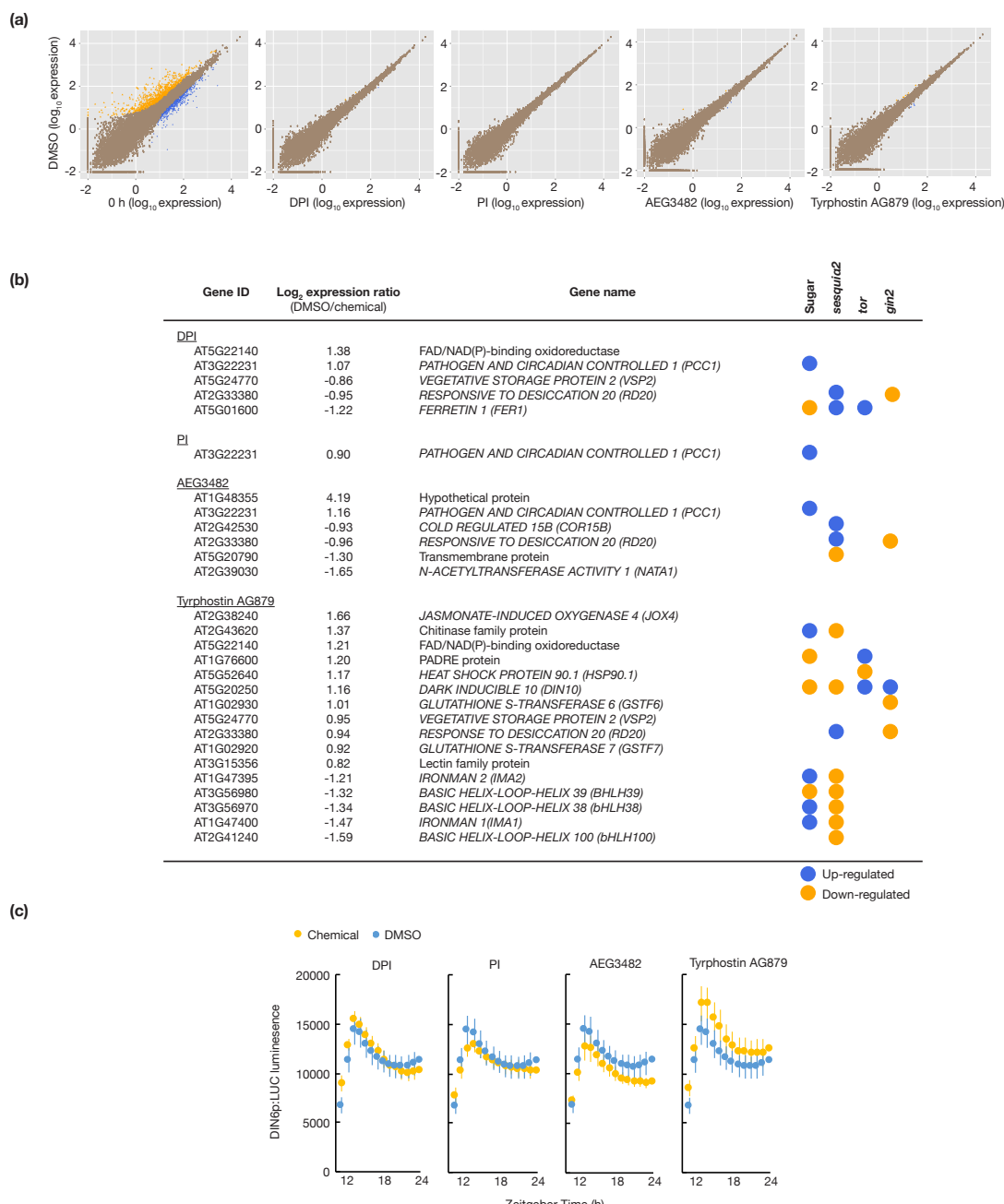
774

775 Figure S5. Effect of chemicals on germination of dormant seeds. Imbibed Col-0 seeds were  
776 sown on  $\frac{1}{2}$  MS containing 30 mM mannitol or 30 mM sucrose containing DMSO or indicated  
777 concentration of chemical (means  $\pm$  SD of four replicate each of 20-25 seeds).



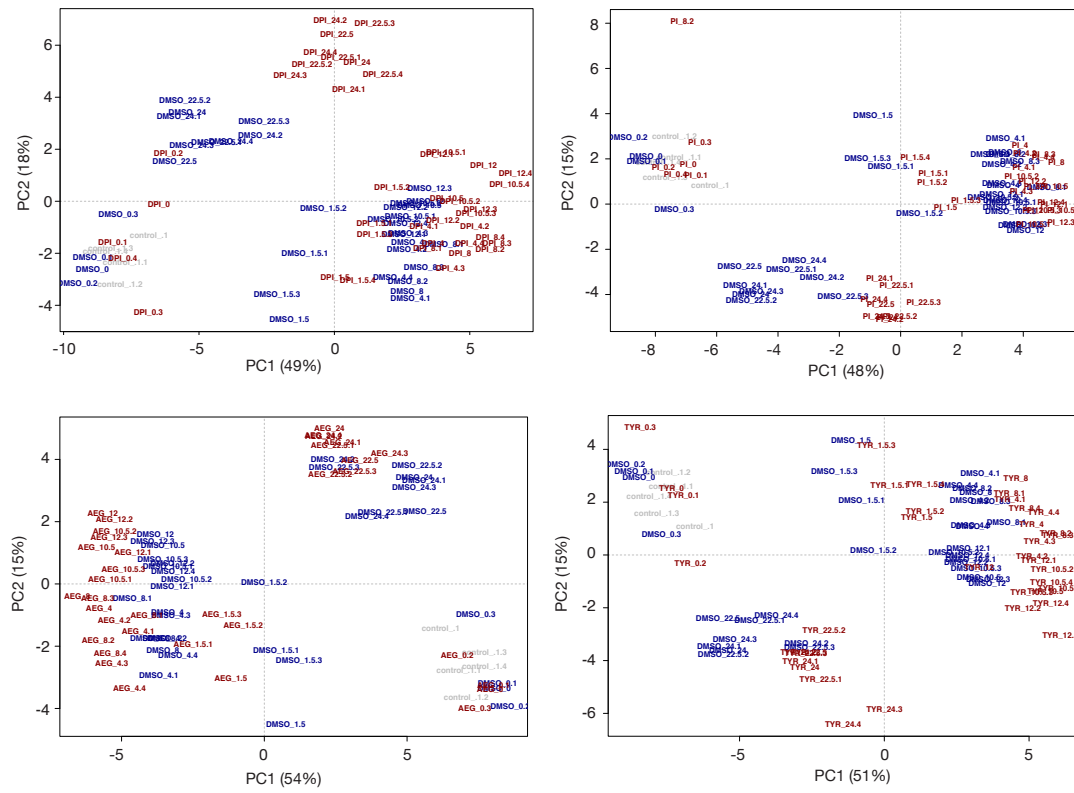
778

779 Figure S6. Effects of chemicals on growth and pigments. (a) Images, (b) fresh weight and (c)  
780 total chlorophyll of 7 d old seedlings grown on  $\frac{1}{2}$  MS containing DMSO or minimum  
781 effective concentration of each chemical (n=4). (d) Hypocotyl length and (e) root length of 7  
782 d old seedlings grown in the dark for 5 d on 30 mM mannitol (blue) or sucrose (red)  
783 containing DMSO or chemical (n=10). (f) Anthocyanin content of 9 d old seedlings grown  
784 for 2 d on 90 mM mannitol (blue) or sucrose (red) with DMSO or chemical (n=4). \* Different  
785 from control (DMSO) by Bonferroni-corrected *t*-test, p < 0.05.



786

787 Figure S7. Effect of selected chemicals on transcriptome at dawn. (a) Comparison of gene  
 788 expression in untreated seedlings at ZT0 (0 h) or after 2 h treatment with DMSO, DPI, PI,  
 789 AEG3482 or Tyrphostin AG879. (b) List of differentially expressed genes between DMSO or  
 790 chemical-treated seedlings. Genes previously identified as differentially expressed in dark-  
 791 adapted seedlings treated with sucrose (Sugar; Román et al 2021) or in mutants of SnRK1  
 792 (*sesqui*; Peixoto et al 2021), TOR (*tor*; Xiong et al 2013) or HXK1 (*gin2*; Ganpudi et al  
 793 2019) are indicated by yellow (down-regulated) or blue (up-regulated). (c) Luciferase  
 794 luminescence in *DIN6p:LUC* seedlings treated with DMSO or chemical before dusk (ZT11)  
 795 (means  $\pm$  SEM, n = 6).



796

797 Figure S8. Principle component analysis of effects of chemicals on primary metabolites.  
798 Principle component 1 (PC1) versus PC2 plots for 63 metabolites measured in untreated  
799 seedlings at ZT0 or seedlings treated with DMSO, DPI, PI, AEG3482 (AEG) or Tyrphostin  
800 AG879 (TYR) and sampled at ZT0, ZT1.5, ZT4, ZT8, ZT10.5, ZT12, ZT22.5 and ZT24.  
801 Each point represents one of five biological replicates.

802

803

804 Table S1. Primers used in this study.

805 Table S2. LOPAC chemicals that modify *CCR2p:LUC* reporter response to sucrose, SSMD  
806  $\pm 1$ .

807 Table S3. DEGs identified by RNA-seq in untreated seedlings or seedlings treated with  
808 DMSO, DPI, PI, AEG3482 or Tyrphostin AG879.

809 Table S4. Metabolite profiling in untreated seedlings or seedlings treated with DMSO, DPI,  
810 PI, AEG3482 or Tyrphostin AG879.